TECHNICAL UNIVERSITY OF CRETE

School of Production Engineering and Management

Movement Strategies for Connected and Automated Vehicles in Lane-free Traffic using Optimal Control

DIPLOMA THESIS

by

Ioannis Faros

supervisor

Prof. Ioannis Papamichail

A thesis submitted in fulfillment of the requirements for the diploma of
Production Engineering and Management
in the

Dynamic Systems and Simulation Laboratory

Chania, Greece
July 2022

This page is intentionally left blank.

THESIS APPROVAL

Author: _____

Ioannis Faros

Committee approvals: _____

Professor Ioannis Papamichail - Thesis Supervisor

_____

Assistant Prof. Eleftherios Doitsidis - Committee Member

_____

Associate Prof. Georgios Chalkiadakis - Committee Member

ABSTRACT

In a variety of fields, automation has enhanced production and reduced errors to a large extent. Automation in vehicular traffic using fully Connected and Automated Vehicles (CAVs) is projected to provide similar outcomes. However, issues such as road safety, human-inspired driving and related road rules result in reduced road usage and loss of traffic flow. Automated vehicles, aided by vehicle-to-vehicle and vehicle-to-infrastructure communication, have the potential to improve safety and traffic flow significantly, by relaxing the road rules designed for human drivers.

According to a recently proposed novel traffic paradigm, called TrafficFluid, there is no need to duplicate the human lane-based driving task. The future of road driving is moving towards complete automation and cooperation among the CAVs. Advanced vehicle sensors and communications, enable the CAVs to "float" securely and efficiently, restoring lost capacity and enhancing traffic safety on various types of roadways, based on appropriate movement tactics.

Alongside various strategies, a nonlinear Optimal Control Problem (OCP) for CAV path planning with nudging in a lane-free traffic environment, as well as, a feasible direction algorithm for its computationally efficient numerical solution are considered. The OCP considers an objective function to minimize fuel consumption, improve passenger comfort, reach desired speeds on both longitudinal and lateral directions, and avoid obstacles. State-dependent bounds on control inputs are used to ensure that the vehicles stay within the road boundaries and prevent crashes in emergency situations. The OCP is solved repeatedly for short time horizons within a model predictive control framework, while the vehicle advances. The proposed approach is shown to give good results in a traffic simulation with wide range of vehicle densities on a lane-free ring-road and can be considered a contender for use in future advancements, linked to lane-free CAV traffic.

Towards this direction, in this thesis, a lateral positioning stratery is developed for reaching the desired lateral position according to the desired longitudinal speed. The strategy is aiming at improving longitudinal vehicle speeds and thereby the traffic mean speed and flow, mainly at under-critical traffic densities, where vehicle maneuvering is easier. This is to be achieved by distributing laterally the vehicles based on their longitudinal desired speeds, so that vehicles with higher desired speed tend to drive further left (and vice versa). Firstly, the desired lateral position is selected based on the distribution of the desired longitudinal speeds. Afterward, the

desired lateral speed of each vehicle is calculated and applied in real-time, as it depends on its actual lateral position. The work leverages the OCP formulation to find an optimal and efficient way to move the CAVs to a desired lateral position and remain there, avoiding crashes. Various densities are being considered for two scenarios on a ring-road for comparative analysis. The proposed strategy is being simulated in a lane-free environment using a custom-made extension, namely TrafficFluid-Sim, which is built for SUMO (Simulation of Urban MObility) simulator. Several quantities, like the average traffic flow and statistical measures of the error in the lateral direction, are calculated for evaluation.

ΠΕΡΙΛΗΨΗ

Σε διάφορους τομείς, ο αυτοματισμός έχει βελτιώσει την παραγωγή και έχει μειώσει τα σφάλματα σε μεγάλο βαθμό. Η οδήγηση με πλήρως αυτοματοποιημένα οχήματα, προβλέπεται να παρέχει παρόμοια οφέλη. Ωστόσο, ζητήματα όπως η οδική ασφάλεια, οι περιορισμένες ανθρώπινες δυνατότητες και κανόνες κυκλοφορίας έχουν ως αποτέλεσμα τη μειωμένη χρήση της χωρητικότητας του δρόμου. Τα αυτόματα οχήματα, με τη βοήθεια της επικοινωνίας όχημα-με-όχημα και όχημα-με-τις οδικές υποδομές, έχουν τη δυνατότητα να βελτιώσουν σημαντικά την οδική ασφάλεια και τη ροή της κυκλοφορίας, εξαιρώντας ή χαλαρώνοντας τους οδικούς κανόνες που έχουν σχεδιαστεί για οδηγούς.

Σύμφωνα με ένα καινοτόμο μοντέλο κυκλοφορίας που προτάθηκε πρόσφατα και ονομάζεται TrafficFluid, δεν υπάρχει ανάγκη να αντιγράψουμε την ανθρώπινη οδήγηση σε λωρίδες. Το μέλλον της οδήγησης κινείται προς την πλήρη αυτοματοποίησή της με τη πλήρη συνεργασία των οχημάτων. Οι προηγμένοι αισθητήρες οχημάτων και η ανάπτυξη των επικοινωνιών επιτρέπουν σε κάθε όχημα να ελίσσεται με ασφάλεια και αποτελεσματικότητα μεταξύ των άλλων, αποκαθιστώντας τη χαμένη χωρητικότητα και ενισχύοντας την ασφάλεια κυκλοφορίας σε διάφορους τύπους δρόμων, με βάση τις κατάλληλες στρατηγικές κίνησης.

Μεταξύ άλλων προσεγγίσεων, η παρούσα εργασία ακολουθεί ένα μη γραμμικό Πρόβλημα Βέλτιστου Ελέγχου (ΠΒΕ) για τον σχεδιασμό της διαδρομής ενός τέτοιου οχήματος σε δρόμο χωρίς λωρίδες. Με αυτή την προσέγγιση, κάθε όχημα έχει τη δυνατότητα να ωθεί με ασφάλεια άλλα οχήματα (nudging) προκειμένου να κινηθεί ταχύτερα. Ένας αλγόριθμος εφικτής κατεύθυνσης χρησιμοποιείται για την αποδοτική αριθμητική επίλυση του προβλήματος. Το ΠΒΕ κάνει χρήση μιας αντικειμενικής συνάρτησης που ελαχιστοποιεί την κατανάλωση καυσίμου, βελτιώνει την άνεση των επιβατών, επιτυγχάνει επιθυμητές ταχύτητες καταμήκος και εγκάρσια, και αποφεύγει τα εμπόδια. Γίνεται χρήση των μεταβλητών κατάστασης στους περιορισμούς στην είσοδο του ελέγχου για να διασφαλιστεί ότι τα οχήματα παραμένουν εντός των ορίων του δρόμου και αποτρέπουν ατυχήματα σε καταστάσεις έκτακτης ανάγκης. Το ΠΒΕ επιλύεται επαναληπτικά καθώς το όχημα κινείται, στο πλαίσιο του προβλεπτικού ελέγχου. Αποδεικνύεται ότι η προτεινόμενη προσέγγιση δίνει καλά αποτελέσματα, σε προσομοίωση κυκλοφορίας, με μεγάλο εύρος τιμών πυκνότητας οχημάτων, σε έναν περιφερειακό δρόμο χωρίς λωρίδες. Η μέθοδος αυτή μπορεί να θεωρηθεί υποψήφια για χρήση - στο μέλλον - σε κυκλοφορία συνδεδεμένων αυτόματων οχημάτων σε δρόμο χωρίς λωρίδες.

Προς αυτή την κατεύθυνση, στην παρούσα διπλωματική εργασία, προτείνεται μια μέθοδος για την επίτευξη της επιθυμητής εγκάρσιας θέσης θεωρώντας ως δεδομένο, την επιθυμητή ταχύτητα του

οχήματος. Η μεθοδος στοχεύει στην αύξηση της ταχύτητας των οχημάτων και κατά συνέπεια στη βελτίωση της κυκλοφοριακής ροής και της μέσης ταχύτητας αυτής. Η επίδραση της μεθόδου είναι εμφανέστερη, σε πυκνότητες κυκλοφορίας μικρότερες από την κρίσιμη, όπου ένα όχημα κινείται ευκολότερα. Αυτό επιτυγχάνεται κατανέμοντας τα οχήματα - κατά το πλάτος του δρόμου - μέ τέτοιο τρόπο, ώστε όσο μεγαλύτερη είναι η επιθυμητή τους ταχύτητα, τόσο αριστερότερα του δρόμου να κινούνται. Αρχικά, η επιθυμητή εγκάρσια θέση επιλέγεται με βάση την κατανομή των (διαμήκων) επιθυμητών ταχυτήτων. Στη συνέχεια, υπολογίζεται και εφαρμόζεται η επιθυμητή εγκάρσια ταχύτητα του κάθε οχήματος σε πραγματικό χρόνο, καθώς εξαρτάται από την τρέχουσα εγκάρσια θέση του. Η εργασία αξιοποιεί τη διατύπωση του ΠΒΕ για να βρεί ένα βέλτιστο και αποδοτικό τρόπο να μετακινηθούν και να παραμείνουν τα οχήματα στην επιθυμητή εγκάρσια θέση τους, αποφεύγοντας παράλληλα τις συγκρούσεις. Εξετάζονται διάφορες πυκνότητες κυκλοφορίας για δύο σενάρια, σε μια περιφερειακή οδό για συγκριτική ανάλυση. Οι προτεινόμενες στρατηγικές προσομειώνονται σε περιβάλλον χωρίς λωρίδες, χρησιμοποιώντας μια προσθήκη κώδικα σε C/C++ - το TrafficFluid-Sim - το οποίο δημιουργήθηκε για τον προσομοιωτή SUMO (Simulation of Urban Mobility). Τέλος, υπολογίζονται μεγέθη, όπως η ροή κυκλοφορίας και στατιστικές εκφράσεις του σφάλματος στην εγκάρσια κατεύθυνση, προκειμένου να αξιολογηθεί η μέθοδος.

ACKNOWLEDGEMENTS

LIST OF FIGURES

LIST OF TABLES

CONTENTS

CHAPTER 1

INTRODUCTION

1.1 Motivation

Connected and Automated Vehicles (CAVs) are predicted to populate the roads in the near future, without the need for human driving. Similar to the automation in the manufacturing sector, CAVs have the potential to revolutionise the transportation sector by using the infrastructure very efficiently and overcoming the sensory limitation of human driving. Human drivers generally compensate the limitations of sensory feedback by using intelligence and learning. With appropriate algorithms, CAVs can outperform the human drivers without the need for the majority of traffic rules. For example, lanes were introduced to help the human drivers by minimizing the lateral monitoring, however, they are designed to fit the widest vehicle, resulting in reduced road utilization [5]. Lane changes and overtaking a slow moving vehicle are still a cause for approximately 10% of the collisions. For making the driving task easier and safer, there have been attempts to use modern automation technologies like vehicle-to-vehicle (V2V) or vehicle-to-infrastructure (V2I) communication for appropriate message passing to the drivers [6]-[7]. However, majority of the road accidents occur due to bad decisions, low perception, and limited driving skills of the human drivers [8]. According to the statistics, 1.3 million people lose their lives every year [9] due to road accidents. Simultaneously, another significant problem is the traffic congestion that requires radical solutions, especially in rush hours [10].

On the other hand, while we are moving on to an era of full automation, one possible solution is the 100% penetration of CAVs, with the essential movement strategies in both lateral and longitudinal direction. When there are no human drivers, the road rules can either be relaxed or ignored. Also, CAVs have the potential of increasing safety, and traffic flow, reducing emissions, as well as, to lead to the economic development. However, because of the the vehicular traffic nature, complex algorithms like nonlinear feedback control, and artificial intelligence techniques like reinforcement learning, are required in order to make decent decision [3].

For future traffic with only CAVs on roads, an unconventional concept, called TrafficFluid, has been proposed. The general car-following models use lanes and also assume that the traffic is anisotropic in nature, where the driver is influenced only by the downstream vehicles. The movement strategies in TrafficFluid have two major differences compared to the conventional car-following models. The first one is a road without lanes, where the vehicles can "float" in

1

a 2-D plane. The second one is vehicle nudging, whereby the vehicles apply some pressure on the downstream vehicles, resulting in some form of isotropy in the traffic. In an era of CAVs, there is no need to follow the traffic rules designed for human drivers. With appropriate design of movement strategies, lanes, traffic signals and many other traffic rules can be removed or relaxed for the CAVs. Furthermore, there are some advantages of a lane-free environment and nudging, like increased capacity, and smoother movement [3].

Considering the principle, in which, vehicles have the appropriate ability to communicate among each other, in the research so far, there have been contributions in the areas like, the internal boundary control [11]-[12], and path planning. Assuming this, the present work, is based an optimal path planning algorithm for CAVs. In [13], as well as in a recently submitted paper [14] a nonlinear constrained Optimal Control Problem (OCP) for the movement of the CAVs in the lane-free environment is proposed. A feasible direction algorithm (FDA) [15], [16] is used to solve the OCP in a Model Predictive Control (MPC) framework [17], [18] in real time and this approach is applied for each vehicle separately. Simulation results for different cases are provided to demonstrate working of proposed methodology. All simulations have been done using a lane-free environment based on a custommade extension, namely TrafficFluid-Sim [19], which is built for the SUMO (Simulation of Urban MObility) simulator [20].

1.2   Thesis Objectives

The objective of the thesis is to improve the longitudinal speeds of the vehicles, mainly at intermediate densities, by distributing laterally the vehicles based on their longitudinal desired speeds. This is achieved by developing and implementing a lateral positioning strategy, which leverage the existing optimal control formulation to move the CAVs to appropriate lateral positions, while respecting other, higher-priority sub-objectives, such as avoiding crashes. First, the longitudinal desired speed of each vehicle is mapped to a lateral desired position under the premise "faster vehicles drive farther left". Then, the value of the desired lateral speed is updated in real-time in dependence on the vehicle's actual versus the desired lateral position, letting the optimal control problem, with the given sub-objective priorities, decide on the actual vehicle path. The proposed strategy is applied for different densities and comparative analysis of the results is performed.

1.3   Thesis Outline

This thesis is composed of six chapters. Chapter 1 gives an introduction which describes the current work that relates to the optimal path planning of CAVs in a lane-free environment. After that, Chapter 2 is a brief description of the background that it is required to understand this diploma thesis. A short explanation about the vehicular traffic, the usefulness of CAVs and their advantages is given. Moreover, there is a brief description about the novel paradigm called TrafficFluid, as well as, its advantages compared to the lane-based model. Last but not least, an extensive report is given on the basics of the concept of the discrete-time optimal control, like the problem formulation and the optimality conditions. In Chapter3, the problem formulation and more specifically the objective function, the state-dependent inequality constraints, as well as, the new proposed lateral positioning strategy are presented. This methodology aims to distribute the vehicles laterally based on their longitudinal desired speeds. In addition,

the solution of the OCP is described. Chapter 4 gives a brief description of the extension TrafficFluid-Sim in SUMO. Moreover, it describes the scenarios and the cases of each scenario that have been used. Chapter 5 summarizes the results. Different kinds of vehicles have been used, like small, normal or big cars, as well as trucks. The last chapter, refers to the conclusions and gives a short summary of the strategy and the findings of this diploma thesis.

CHAPTER 2

BACKGROUND

Chapter 2 presents the basic concept and ideas of traffic systems nowadays. Section 2.1 refers to the concept of Vehicle Automation and Communication Systems. Section 2.2 gives a short explanation about Connected and Automated Vehicles (CAVs) and their impact. Furthermore, sections 2.3 & 2.4 explain the TrafficFluid paradigm and compare it with the conventional road type. The last section 2.5, gives a brief explanation of the theory of discrete-time optimal control.

2.1 Vehicular Traffic

Vehicular traffic plays an important role for the transport of persons and goods and enhances the economic and social life of a modern society. However, even after decades of research, issues like traffic congestion and accidents appear in everyday life, especially in urban areas around the globe, and call for radical solutions. Some of the traffic congestion consequences are travel delays, slow down of certain emergency services like fire and ambulance, and excessive fuel consumption due to non-smooth movement of vehicles. Although the conventional traffic management has valuable results, it cannot completely counter the heavy traffic congestion or accidents. In the direction of resolving aforementioned issues, there has been an important effort to develop a variety of both Vehicle Automation and Communication Systems (VACS) and control strategies in the last few years, that are expected to improve the capabilities of the individual vehicles [21].

2.1.1 VACS

VACS are systems that transform some of the vehicle functions at various levels of automation ranging from basic driver assistance to full automation. Simultaneously, the mobile communication industry has achieved some of the most important innovations and has changed the lifestyle. The use of the advanced mobile communication systems in vehicles is projected to provide serious changes in transportation technology. Moreover, the communications systems in VACS allow a varying levels of cooperation enabling vehicle-to-vehicle (V2V) and vehicle-to-infrastructure (V2I) communication. Furthermore, a variety of companies and research institutions have been working on technological advances to improve the driving conditions for

both driver and passenger. Recently, a lot of researchers and industries are working and testing fully automated vehicles using methodologies such as Artificial Intelligence (AI), optimal control, and reinforced learning in order to measure the decisions about the car-following and lane changing [22], [3].

2.1.2 The Need for Traffic Control

As mentioned earlier, one of the biggest challenges for traffic control is managing congestion phenomena. Control strategies have been developed in a lane environment in order to solve problems like congestion and consequently to provide a safer, a more efficient and less polluting transportation. The effectiveness of traffic control depends on the quality of the control strategies, so the development of efficient traffic control methodologies has a major social impact and requires great responsibility [23]. Figure 2.1 displays a general scheme of the feedback control for a traffic system. The control inputs are calculated by the traffic controller and transferred as input to the traffic system. The exogenous inputs such as types of vehicles affect the system, however these exogenous inputs are measurable and detectable. The traffic controller includes the control algorithm, which can be applied to the vehicles. Last but not least, the feedback loop has the measurements, such as speeds, obstacles, and decision of the other vehicles [1].
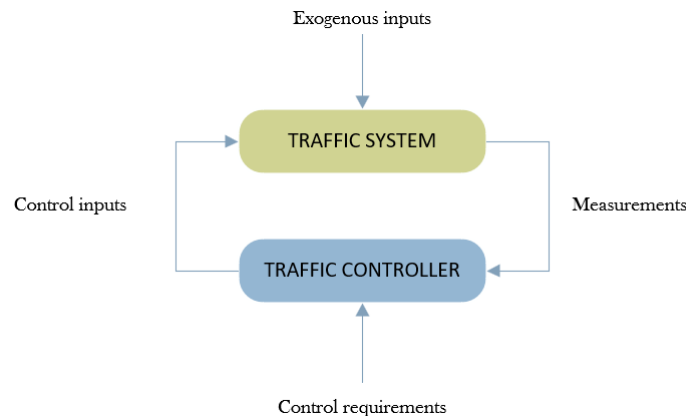
Figure 2.1: Traffic controller, Source: [1]

2.2 Connected and Automated Vehicles

From nonmotorized transportation to a high-speed roadway network with modern vehicle technologies, the transportation sector has progressed. The goal is to transition from traditional transportation engineering practices, to implementing emerging technologies, primarily because these technologies have the potential to eliminate the human role in certain decision-making situations and provide the necessary alerts and warnings to help drivers and road users to improve their safety [24]. Modern type of transport vehicles like cars without drivers or standalone vehicles are in the peak of technology. Control systems with a set of sensors and actuators, as well as, the navigation process that combine several steps to obtain all the sufficient data in order to generate a path without collisions, are the essential features of the modern transportation systems. So, Automated Vehicles (AVs) steer, accelerate, and brake with little or no

human intervention. Some vehicles still require human assistance to keep an eye on the road, while others do not [25].

On the other hand, networking facilities such as communications devices of novel wireless connections e.g 5G, allow vehicles to communicate and to transfer information among the road elements like vehicles, traffic light etc. All these interconnected processing, sensing and communication capabilities contribute to the control of the intelligent vehicles. The connected vehicles communication systems are classified into the three following categories [2]:

- **V2V**: an architecture that allows a direct communication between the vehicles without any fixed infrastructure support

- **V2I**: communication with the road infrastructure such as traffic lights, signs, and other roadside objects

- **Hybrid architecture**: a combinations of both V2V and V2I solutions
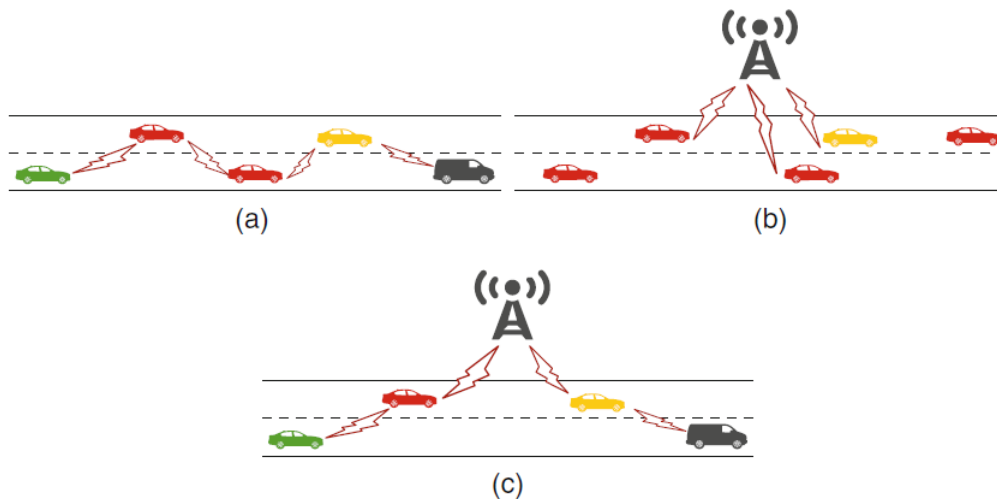
Figure 2.2: (a) Vehicle to Vehicle, (b) Vehicle to Infrastructure, (c) Hybrid architecture, Source: [2]

So, CAVs technology can be used to achieve the following objectives: [24]

Safety

According to the National Highway Traffic Safety Administration, 94 - 96% of traffic collisions are caused by human error. For this reason, a drastic improvement in traffic safety is essential to reduce the human error. CAVs can be a solution to the issue, where the human error is completely eliminated. Although, a lot of vehicle-centric applications are in market like lane departure warning system, speed updates, such technologies only help the human drivers to some extent and we still have accidents due to human negligence. The research now is on the introduction of CAVs on roads and further to use a lane-free environment in a traffic without

human drivers. So, considering the potential of CAVs technologies in order to improve safety, it is irrational not using them.

Mobility

In the near future, CAVs have the potential to change the way people travel. CAVs technologies are able to detect incidents like rapid surge or increase in vehicular speeds or rising vehicular volumes. However, the most important thing is that the communication between CAVs and emergency technologies can help incident responders to reach their location not only quickly, but also clear from the roadway traffic.

Environment

In United States the transportation is the primary source of carbon emissions. By saving fuel and decreasing emissions, emerging and CAVs technologies can help to reduce the carbon footprint and promote green transportation choices. On the other hand, the impact of CAVs should also be evaluated because they also have the potential to increase fuel consumption due to higher travel speeds and increased travel.

Economic Development

In the context of CAVs technologies, the society leads to an economic development. Increased safety, better mobility and improved environmental quality lead to better public health and sustainable productivity. Although, the impact of this technology in economic sector is not direct and difficult to quantify, trustworthy transportation network plays an important role in the financial welfare of the society, as well as, offers a better quality of life of all road users.

2.3   TrafficFluid

A novel paradigm, called TrafficFluid, has been proposed in order to study movement control strategies for various type of vehicles and sizes e.g. cars, vans, trucks etc in a new road environment [3].The paradigm proposes the following two principles:

- Lane-free Traffic

- Nudging

2.3.1   Lane-Free Traffic

In lane-free traffic vehicles are not restricted to traffic lanes, as in traditional traffic, but may drive wherever on the road's 2-D surface, subject to the road's borders and avoiding collisions. According to the figure 2.3, the road has no lanes and the percentage "%" on each vehicle represents their actual speed as a percentage of their desired. Vehicles colored yellow have actual speed less than their desired and vice-versa for the blue ones. In a lane-free environment,

the CAVs can be considered as particles, which constitutes an artificial fluid. Here, vehicle movement strategies may be influenced by the vehicles behind the ego, something which is called "nudging" and it is explained below. [3]
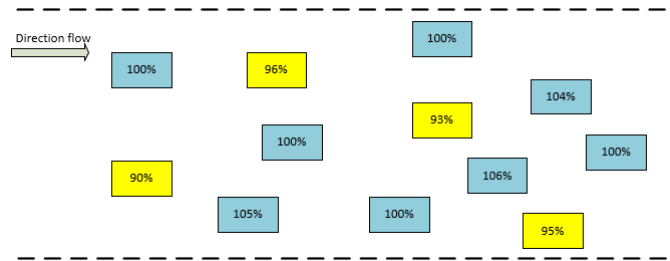
Figure 2.3: Lane free environment, Source: [3]

2.3.2 Nudging

The nudging effect accomplishes among vehicles which communicate, and its purpose is to "push" the slower vehicles, which are in the way of ego, to pass. According to the figure 2.4, the yellow vehicle has bigger longitudinal speed than the blue ones, and for this reason nudges the slower vehicles aside to pass. [3]
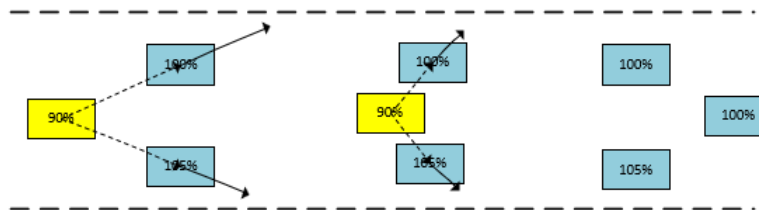
Figure 2.4: Nudging effect, Source: [3]

2.4   Lane-Based vs Lane-Free Traffic

The lane-based traffic was introduced in order to make the driving task easier for the human drivers. Firstly, lane markings on roads and highways were needed to separate opposing traffic directions to minimize the danger of head-on crashes, while the dashed lines are dividing parallel lanes in the same traffic direction. In manual driving, parallel lanes improve traffic safety by simplifying the driving task for the human driver; when driving in a lane, the driver just needs to check the distance and speed of the front car, while there is little need to monitor the left, the right, and the rear sides of his or her own vehicle. Generally, two primary considerations control driving tasks [5]:

- maintaining desired speeds;

- staying in a lane or overtake slower vehicle

Due to the wide range of vehicle widths e.g cars, trucks, and motorcyclists, as well as the need for safety margins, lane-based traffic must waste a portion of the available road width to fit the widest vehicle, and hence the possible capacity. Furthermore, during the lane changing of a vehicle, the freeway's capacity and safety are reduced. In addition, one-tenth of all accidents are caused by improper lane changes. For this reason, developing movement strategies in order to avoid crashes during lane changes requires understanding human driver behavior, which differs from person to person due to the limited perception of sense and the reaction time of decision-making [3], [5]. In the lane-based environment, even CAVs face difficulties in lane changing due to large trajectory calculations [26], [27]. However, some possible solutions have been proposed, like complex algorithms and optimization techniques [28]. Moreover, there have been suggested methods, like nonlinear feedback control for collision avoidance [29], and artificial intelligence methods, like deep learning, where autonomous vehicles try to avoid obstacles and advance smoothly [30].
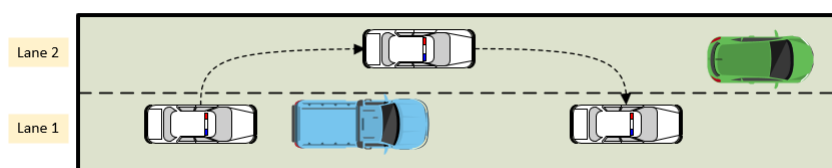
Figure 2.5: Lane-changing in lane-based environment

On the other hand, in the era of full automation, there is no need to duplicate human driving behavior. In the near future, the driving task on road will be completely automated, and with the combination of high-level sensors and communications, the capabilities of driving will be highly increased. All these capabilities in a lane-free environment will allow the CAVs to "float" safely on different types of roads like highways, motorways, and arterials. The lost capacity will be regained, safety will be increased and of course, the movement strategies will be designed easier and more efficiently due to 2-D vehicle movement. Figure 2.6 illustrates the most important advantages of lane-free traffic. The movement strategies may differ according to various characteristics of infrastructures and vehicles, but they will have an important impact on efficiency. In the research done so far, various strategies have been proposed in a lane-free

environment, in order to advance the vehicles securely, avoiding parallel collisions. Techniques, like reinforcement learning [31], Optimal Control (OC) and Model Predictive Control (MPC) solutions for an optimized path planning of CAVs have been proposed [13]. Towards this direction, the current work relates with [13], while trying to find an efficient method for the lateral movement of the CAVs, so as to distribute the vehicles laterally based on their longitudinal desired speeds. The solution to this problem comes across with a Feasible Direction Algorithm (FDA) -which produces feasible trajectories for the CAVs- in an MPC framework in the general context of an OCP.
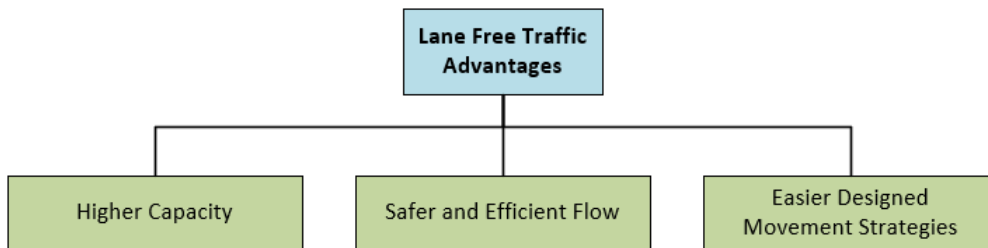
Figure 2.6: Lane-free advantages

2.5 The Theory of Discrete-Time Optimal Control

The optimal control theory was established around 1960s for both continue and discrete time systems. A big variety of applications of optimal control in different technical areas were reported, particularly in the area of space technology, robotics and transportation.

2.5.1 Problem Formulation

The discrete-time problem formulation uses the following cost criterion for minimization:

$$J = \theta[\boldsymbol{x}(K)] + \sum_{k=0}^{K-1} \phi[\boldsymbol{x}(k), \boldsymbol{u}(k), k] \tag{2.1}$$

subject to the constraints:

$$\boldsymbol{x}(k+1) = \boldsymbol{f}[\boldsymbol{x}(k), \boldsymbol{u}(k), k], k = 0, ..., K-1 \tag{2.2}$$

$$x(0) = x_0 \tag{2.3}$$

$$\boldsymbol{h}[\boldsymbol{x}(k), \boldsymbol{u}(k), k] \leq \boldsymbol{0}, k = 0, ..., K-1 \tag{2.4}$$

and the final condition:

$$\boldsymbol{g}[\boldsymbol{x}(K)] = \boldsymbol{0} \tag{2.5}$$

Equation 2.2 refers to the state equation discribing the dynamic process, where $\boldsymbol{x} \in \mathrm{R}^n$ is the system state variable vector, and $\boldsymbol{u} \in \mathrm{R}^n$ is the control variable vector. The $\boldsymbol{f} \in \mathrm{R}^n$ is a twice continuous differentiable vector function. Furthermore, k is the discrete time index which is connected with the continuous time with $t = kT$, where T is the sample time interval, and K is the fixed time horizon. Equation 2.3 refers to the initial state, while equation 2.4 refers to inequality constraints, where $\boldsymbol{h}, \phi$ and $\theta \in \mathbb{R}^q$ are twice continuous differentiable functions. Last but not least, the final condition may be free or may be required to satisfy equation 2.5, where $\boldsymbol{g} \in \mathbb{R}^l, l \leq n$, is a twice continuous differentiable vector function.

To see this problem formulation from a more "optimization" point of view, it is required to define the vectors:

$$\boldsymbol{X} = [x(1)^T...x(K)^T]^T \tag{2.6}$$

$$\boldsymbol{U} = [\boldsymbol{u}(1)^T...\boldsymbol{u}(K)^T]^T \tag{2.7}$$

The discrete-time optimal control problem may be expressed in a more optimization way as:

Minimize $\Phi(\boldsymbol{X}, \boldsymbol{U})$

subject to

$$\boldsymbol{F}(\boldsymbol{X}, \boldsymbol{U}) = \boldsymbol{0}, \boldsymbol{H}(\boldsymbol{X}, \boldsymbol{U}) \leq \boldsymbol{0}$$

where Φ is the cost function, $\boldsymbol{H}$ the inequality constraints and $\boldsymbol{F}$ the state equation for all $k \in [0, K-1]$ and the terminal condition 2.5.

2.5.2 Optimality Conditions

In order to derive the optimality conditions, the Lagrangian Function for this problem is constructed:

$$L[\boldsymbol{x}(k), \boldsymbol{u}(k), \boldsymbol{\lambda}(k), \boldsymbol{\mu}(k), \boldsymbol{v}, k] = \theta[\boldsymbol{x}(K)] + \sum_{k=0}^{K-1} \phi[\boldsymbol{x}(k), \boldsymbol{u}(k), k] +$$

$$\sum_{k=0}^{K-1} \boldsymbol{\lambda}(k+1)^T [\boldsymbol{f}[\boldsymbol{x}(k), \boldsymbol{u}(k), k] - \boldsymbol{x}(k+1)] + \boldsymbol{\mu}(k)^T \boldsymbol{h}[\boldsymbol{x}(k), \boldsymbol{u}(k), k] + \boldsymbol{v}^T \boldsymbol{g}[\boldsymbol{x}(K)] \qquad (2.8)$$

The Lagrangian Function consists of the cost function 2.1, the state equations 2.2 multiplied by the **Lagrange multipliers**, $\boldsymbol{\lambda}(k+1) \in \mathbb{R}^n$, the inequalities 2.4 multiplied by the **Kuhn-Tucker multipliers**, $\boldsymbol{\mu}(k) \in \mathbb{R}^q$ and the final condition 2.5 multiplied by the $\boldsymbol{v} \in \mathbb{R}^n$ multipliers.

In more comprehensive form, equation 2.8 can be written:

$$L[\boldsymbol{x}(k), \boldsymbol{u}(k), \boldsymbol{\lambda}(k), \boldsymbol{\mu}(k), \boldsymbol{v}, k] = \Phi(\boldsymbol{X}, \boldsymbol{U}) + \boldsymbol{\Lambda}^T \boldsymbol{F}(\boldsymbol{X}, \boldsymbol{U}) + \boldsymbol{M}^T \boldsymbol{H}(\boldsymbol{X}, \boldsymbol{U}) \qquad (2.9)$$

Applying the necessary conditions of optimality:

$$\frac{\partial L}{\partial \boldsymbol{X}} = 0 \qquad (2.10a)$$

$$\frac{\partial L}{\partial \boldsymbol{U}} = 0 \qquad (2.10b)$$

$$\frac{\partial L}{\partial \boldsymbol{\Lambda}} = 0 \qquad (2.10c)$$

$$\boldsymbol{H}(\boldsymbol{X}, \boldsymbol{U}) \leq \boldsymbol{0} \qquad (2.10d)$$

$$\boldsymbol{H}^T \boldsymbol{M} = 0 \qquad (2.10e)$$

$$\boldsymbol{M} \geq \boldsymbol{0} \qquad (2.10f)$$

derive the necessary conditions of optimality for the discrete-time optimal control problem. These conditions are usually expressed in terms of the -extended- **Hamiltonian Function** as it follows:

$$\hat{H}[\boldsymbol{x}(k), \boldsymbol{u}(k), \boldsymbol{\lambda}(k), \boldsymbol{\mu}(k), k] = \phi[\boldsymbol{x}(k), \boldsymbol{u}(k), k] + \boldsymbol{\lambda}(k+1)^T \boldsymbol{f}[\boldsymbol{x}(k), \boldsymbol{u}(k), k] + \boldsymbol{\mu}(k)^T \boldsymbol{h}[\boldsymbol{x}(k), \boldsymbol{u}(k), k]$$
$$(2.11)$$

Then the necessary conditions of optimality for the optimal control problem are (notation $\boldsymbol{x}_y = \partial \boldsymbol{x} / \partial y$):

$$x(k+1) = \frac{\partial \hat{H}}{\partial \boldsymbol{\lambda}(k+1)} = \boldsymbol{f}[\boldsymbol{x}(k), \boldsymbol{u}(k), k] \tag{2.12a}$$

$$\lambda(k) = \frac{\partial \hat{H}}{\partial \boldsymbol{x}(k)} = \phi_{\boldsymbol{x}(k)} + \boldsymbol{f}_{\boldsymbol{x}(k)}^{T}\boldsymbol{\lambda}(k+1) + \boldsymbol{h}_{\boldsymbol{x}(k)}^{T}\boldsymbol{\mu}(k) \tag{2.12b}$$

$$\frac{\partial \hat{H}}{\partial \boldsymbol{u}(k)} = \phi_{\boldsymbol{u}(k)} + \boldsymbol{f}_{\boldsymbol{u}(k)}^{T}\boldsymbol{\lambda}(k+1) + \boldsymbol{h}_{\boldsymbol{u}(k)}^{T}\boldsymbol{\mu}(k) = 0 \tag{2.12c}$$

$$\boldsymbol{\mu}(k)^{T}\boldsymbol{h}[\boldsymbol{x}(k), \boldsymbol{u}(k), k] = 0 \tag{2.12d}$$

$$\boldsymbol{\mu} \geq \boldsymbol{0} \tag{2.12e}$$

$$\boldsymbol{h}[\boldsymbol{x}(k), \boldsymbol{u}(k), k] \leq \boldsymbol{0} \tag{2.12f}$$

In addition, the boundary and transversality conditions must be satisfied:

$$\boldsymbol{x}(0) = \boldsymbol{x}_0 \tag{2.13}$$

$$\boldsymbol{g}[\boldsymbol{x}(K)] = \boldsymbol{0} \tag{2.14}$$

$$\boldsymbol{\lambda}(K) = \theta_{x(K)} + \boldsymbol{g}_{x(K)}^{T}\boldsymbol{v} \tag{2.15}$$

Equations 2.12a and 2.12b are called the state and costate difference equations respectively, and together consist the system of canonical difference equations of the problem.

2.5.3   State-Dependent Control Bounds

The state-dependent control bounds are of the form:

$$\boldsymbol{u}_{min}(\boldsymbol{x}(k), k) \leq \boldsymbol{u}(k) \leq \boldsymbol{u}_{max}(\boldsymbol{x}(k), k) \tag{2.16}$$

where $\boldsymbol{u}_{min}(\boldsymbol{x}(k), k)$ and $\boldsymbol{u}_{max}(\boldsymbol{x}(k), k)$ are twice continuously differentiable functions. The equations in the form of 2.4 may be reduced to 2.16 if the state equation is of the form of 2.2. By replacing the x from the state equation in the inequality constraint and by resolving for $u(k)$, if possible, is obtaining the state-dependent control bound. However, the state dependence of the bounds, needs some further measures in order to guarantee fulfillment of the necessary optimality conditions. By writing the equation 2.16 as:

$$\boldsymbol{h}[\boldsymbol{x}(k), \boldsymbol{u}(k), k] = [\boldsymbol{u}(k) - \boldsymbol{u}_{max}(\boldsymbol{x}(k), k)][\boldsymbol{u}(k) - \boldsymbol{u}_{min}(\boldsymbol{x}(k), k)] \leq \boldsymbol{0} \tag{2.17}$$

occurs the following two equations:

$$\frac{\partial \boldsymbol{h}}{\partial \boldsymbol{x}} \neq \boldsymbol{0} \tag{2.18}$$

$$\frac{\partial \boldsymbol{h}}{\partial \boldsymbol{u}(k)} = 2\boldsymbol{u}(k) - \boldsymbol{u}_{max}(\boldsymbol{x}(k), k) - \boldsymbol{u}_{min}(\boldsymbol{x}(k), k) \tag{2.19}$$

CHAPTER 3

PATH PLANNING FOR CAVS

Chapter 3 presents the problem formulation with all the constraints, the objective function and the solution of the OCP. The paragraph 3.2 describes the lateral positioning strategy that is used in the problem, while the paragraph 3.3 represents the Optimal Control Problem, as well as, the solution.

3.1 Problem formulation

3.1.1 Kinematics and Constraints

This thesis is based on a work by [13], which develops a nonlinear Optimal Control Problem (OCP) with state-dependent constraints in a lane-free environment. At this point, it will be presented from the ground up the methodology, as well as, the further extensions that are took place in this thesis.

The problem consists of a dynamic model with an objective function that needs to be minimized subject to some constraints, in order to achieve some specific features like to move smooth in a lane-free environment without collisions. Each vehicle is described by four equations, two in the longitudinal direction and two in the lateral direction. The equations are called **state equations** and occur from the laws of kinematics. Firstly, the equations will be written with variables according to classical physics and then will be replaced by other variables in order to seem like an optimization problem. Considering a 2-D plane as well as, discrete time, the following equations are obtained:

$$S_y = S_{0y} + u_y t + \frac{1}{2}t^2 a_y \tag{3.1}$$

$$u_y = u_{0y} + a_y t \tag{3.2}$$

$$S_x = S_{0x} + u_x t + \frac{1}{2}t^2 a_x \tag{3.3}$$

$$u_x = u_{0x} + a_x t \tag{3.4}$$

The equations 3.1-3.2 refer to the lateral direction, while the 3.3-3.4 refer to the longitudinal. The state equations in optimization form for the qth vehicle are the following:

$$x_1^q(k+1) = x_1^q(k) + Tx_3^q(k) + \frac{1}{2}T^2u_1^q(k) \tag{3.5a}$$

$$x_3^q(k+1) = x_3^q(k) + Tu_1^q(k) \tag{3.5b}$$

$$x_2^q(k+1) = x_2^q(k) + Tx_4^q(k) + \frac{1}{2}T^2u_2^q(k) \tag{3.5c}$$

$$x_4^q(k+1) = x_4^q(k) + Tu_2^q(k) \tag{3.5d}$$

According to the state equation 3.5, the state variables $x_1^q, x_2^q, x_3^q, x_4^q$, represent the longitudinal position, the lateral position, the longitudinal speed and the lateral speed, respectively, while the control inputs u_1^q, u_2^q correspond to the longitudinal and lateral accelerations, respectively. Variable T is the time step, which relates with the time through $t = kT$, where k is the discrete-time index. Figure 3.1 displays the variables of a vehicle in the 2-D plane. For each vehicle, at every time horizon, a path generation is required. The path depends on future paths of near vehicles, and this is feasible by the condition, that vehicles communicate among each other via V2V communications.
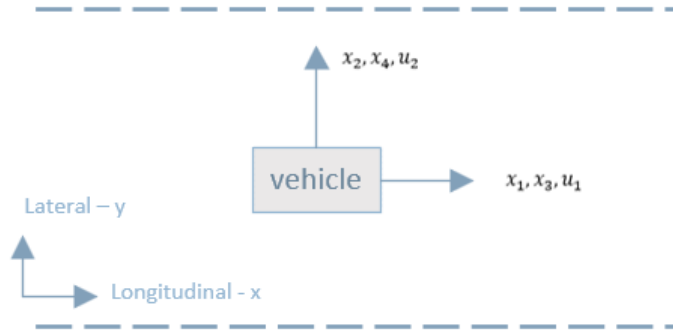
Figure 3.1: Kinematics

The constraints of this problem are about preventing negative longitudinal speeds, avoiding collisions in both directions, and preventing road departures. These constraints are given as state-dependent equation in an inequality form on accelerations.

The general form for the qth constraint in the longitudinal direction is given by the following equation:

$$u_{min1}^q(k) \leq u_1^q(k) \leq u_{max1}^q(k) \tag{3.6}$$

For the lower limit, it is assumed that, the longitudinal speed is non-negative in the time $k+1$, i.e. $x_3^q(k+1) \geq 0$. By replacing the equation 3.5d in 3.6, occurs the following equation:

$$u_1^q(k) \geq -\frac{1}{T}x_3^q(k) \tag{3.7}$$

and hence the state-dependent lower limit is : $U^q_{min1}(k) = \frac{1}{T}x^q_3(k)$. However, due to constrained deceleration capabilities of the vehicle, a constant lower limit is also assumed: U^q_{min1}. Consequently, the lower limit might takes values in:

$$u^q_{min1}(k) = \max\left[U^q_{min1}(k), U^q_{min1}\right] \tag{3.8}$$

With respect to the upper limit for the longitudinal control bound, a constant upper bound U^q_{max1} is defined, due to the constrained acceleration capabilities of the vehicle. On the other hand, the state-dependent constraint for the upper limit is used only in seldom situations, which are about when the OCP returns a collision. If a collision is detected, then the state-depend bound activates. Therefore, a longitudinal position limit is defined, to avoid a crash with the in front vehicle, i.e, the ego vehicle must not cross this limit at k+2 time step. The position limit $\hat{x}^q_1$ has the same meaning as in equation 3.5, and can be written:

$$\hat{x}^q_1(k + 1) = \hat{x}^q_1(k) + T\hat{x}^q_3 + \frac{1}{2}T^2\hat{u}^q_1 \tag{3.9a}$$

$$\hat{x}^q_3(k + 1) = \hat{x}^q_3 + T\hat{u}^q_1(k) \tag{3.9b}$$

Hence, the condition of non-collision is given by the following equation:

$$x^q_1(k + 2) \le \hat{x}^q_1(k + 2) \tag{3.10}$$

If the constraint 3.10 is activated, then ego vehicle should have its longitudinal speed equals to the moving boundary:

$$x^q_3(k + 2) = \hat{x^q_3}(k + 2) \tag{3.11}$$

By replacing in the 3.5a-3.5b and 3.9, where $k = k + 2$, we obtain:

$$x^q_1(k + 2) = x^q_1(k + 1) + Tx^q_3(k + 1) + \frac{1}{2}T^2u^q_1(k + 1) \tag{3.12}$$

$$\hat{x}^q_1(k + 2) = \hat{x}^q_1(k + 1) + T\hat{x}^q_3(k + 1) + \frac{1}{2}T^2\hat{u}^q_1(k1 + 1) \tag{3.13}$$

Substituting equations 3.12 and 3.13, we have the following rearrangements:

$$0 = x^q_1(k + 1) + Tx^q_3(k + 1) + \frac{1}{2}T^2u^q_1(k + 1) - \hat{x}^q_1(k + 1) - T\hat{x}^q_3(k + 1) - \frac{1}{2}T^2\hat{u}^q_1(k1) \tag{3.14}$$

By replacing, where $x^q_1(k+1)$ and $\hat{x}^q_1(k+1)$, their formula from the state equation respectively, the 3.14 can be reduced in:

$$0 = x^q_1(k) - \hat{x}^q_1(k) + 2T[x^q_3(k) - \hat{x}^q_3(k)] + \frac{3}{2}T^2[u^q_1(k) - \hat{u}^q_1(k)] + \frac{1}{2}T^2[u^q_1(k + 1) - \hat{u}^q_1(k + 1)] \tag{3.15}$$

Finally, by using the equation 3.11 and resolving by $u^q_1(k)$ occurs:

$$u^q_1(k) \le -\frac{1}{T^2}[x^q_1(k) - x^q_1\hat{(k)}] - \frac{3}{2T}[x_13^q(k) - x^q_3\hat{(k)}] + u^q_1\hat{(k)} \tag{3.16}$$

The right hand of the equation 3.16 can be considered as a dead beat controller, which can lead the vehicle in exactly two time steps to reach the moving boundaries. In order to avoid this situation, the magnitude of the longitudinal acceleration can be chosen properly by some feedback gain, and then the 3.16 can be replaced by the maximum control input in the longitudinal direction:

$$u_{max1}^q(k) = -K_{long1}e_1^q(k) - K_{long2}e_2^q(k) + \hat{u_1^q}(k) \tag{3.17}$$

where, $K_{long1} \in (0, \frac{T^2}{2}]$, $K_{long2} \in (0, \frac{3}{2T}]$ and e_1^q, e_2^q are the tracking errors.

The gain values of K_{long1} and K_{long2} must be chosen, to result in aperiodic tracking, when the limit is active. By using the 3.5a, 3.5c and 3.17, and after some arraignments, occurs in a matrix form the following:

$$\begin{bmatrix} e_1^q(k+1) \\ e_2^q(k+1) \end{bmatrix} = \begin{bmatrix} 1 - \frac{1}{2}T^2K_{long1} & T - \frac{1}{2}T^2K_{long2} \\ TK_{long1} & 1 - TK_{long2} \end{bmatrix} \begin{bmatrix} e_1^q(k) \\ e_2^q(k) \end{bmatrix} \tag{3.18}$$

The roots of the characteristic equation should be in a unit circle and also be non-negative real, in order to have stability and aperiodic behavior, respectively. So, we choose $K_{long2} = 2\sqrt{K_{long1}} - K_{long1}T/2$, for keeping the design procedure simple, and for letting the roots be non-negative and identical.

To sum up, the upper limit can take two values either $u_{max1}^q(k) = U_{max1}$ or $u_{max1}^q(k) = U_{max1}(k)$ for normal or collision situations, respectively.

According to the lateral constraints, the vehicle should stay within the lateral road boundaries or drive on a road boundary. Moreover, an imaginary boundary is defined, as for the longitudinal direction, in order to avoid collision in the lateral direction. Firstly, the ego vehicle should stay within the road boundaries in the k+2 time step. The k+2 time step is used because the acceleration becomes smoother, when we examine its behavior two time steps in front. So, the lateral position is bounded from equation 3.19, where $\tilde{x}_2^q$ refers to the half of the vehicle's width $(W_v/2)$ and the $\hat{x}_2^q$ refers to the road width minus half of the ego vehicle's width $(W_r - W_v/2)$.

$$\tilde{x}_2^q(k+2) \leq x_2^q(k+2) \leq \hat{x}_2^q(k+2) \tag{3.19}$$

If the ego vehicle cross and stay on the left or on the right side of the road boundary, then the lateral speed of the ego must be set equal to zero i.e. $x_4^q(k+2) = 0$, and from the state equation derives that $x_4^q(k+1) + Tu_2^q(k+1) = 0$. By replacing in 3.5c and 3.5d where $k = k+1$, and after some rearrangements, we obtain:

$$x_2^q(k+1) = x_2^q(k) + Tx_4^q(k) + \frac{1}{2}T^2u_2^q(k) \rightarrow x_2^q(k+2) = x_2^q(k+1) + Tx_4^q(k+1) + \frac{1}{2}T^2u_2^q(k+1) \tag{3.20}$$

$$x_4^q(k+1) = x_4^q(k) + Tu_2^q(k) \rightarrow x_4^q(k+2) = x_4^q(k+1) + Tu_2^q(k+1) = 0 \tag{3.21}$$

In 3.20 by replacing the $x_2^q(k+1)$ with the state equation occurs:

$$x_2^q(k+2) = x_2^q(k) + 2Tx_4^q(k) + \frac{3}{2}T^2u_2^q(k) + \frac{1}{2}T^2u_2^q(k+1) \tag{3.22}$$

17

In the equation 3.22 by replacing the $u_2^q(k+1)$ with the equation 3.21 derives that:

$$x_2^q(k+2) = x_2^q(k) + \frac{3}{2}T x_4^q(k) T^2 u_2^q(k) \tag{3.23}$$

Finally, by replacing the above equation in the inequality 3.19, we obtain the state-dependent constraint:

$$-\frac{1}{T^2}[x_2^q(k) - \tilde{x}_2^q(k+2)] - \frac{3}{2T}x_4^q(k) \leq u_2^q(k) \leq -\frac{1}{T^2}[x_2^q(k) - \hat{x}_2^q(k+2)] - \frac{3}{2T}x_4^q(k) \tag{3.24}$$

Similar to the longitudinal direction, if 3.24 is considered as equality, then works like a deadbeat controller and can lead the ego vehicle in exactly two time steps to the road boundary in the lateral direction. Moreover, the magnitudes resulting from the lateral accelerations, may cause passenger discomfort from high values. For this reason, by choosing the appropriate gains i.e., $K_{lat2} = 2\sqrt{K_{lat1}} - K_{lat1}T/2$, the lateral "controller" remain smoother and get the vehicle asymptotically in the road boundaries, and is given by the following equation:

$$U_{min2}^q(x_2(k), x_4^q(k)) = -K_{lat1}[x_2^q(k) - \tilde{x}_2^q(k)] - K_{lat2}x_4^q(k) \tag{3.25a}$$
$$U_{max2}^q(x_2^q(k), x_4^q(k)) = -K_{lat1}[x_2^q(k) - \hat{x}_2^q(k)] - K_{lat2}x_4^q(k) \tag{3.25b}$$

where $K_{lat1} \in (0, \frac{1}{T^2}]$ and $K_{lat2} \in (0, \frac{3}{2T}]$.

Hence, equation 3.25 can be used either for staying in the road boundaries or in emergency situations, where the ego vehicle and an obstacle is preventing to have a lateral crash.

As before, for consistency of notion it defined the lower and the upper limits as: $u_{min2}^q(k) = U_{min2}^q(k)$ and $u_{max2}^q(k) = U_{max2}^q(k)$.

To sum up, the longitudinal and the lateral control bounds as the shown in 3.8, 3.17 and 3.25 can be expressed by the following state-dependent constraints:

$$h_1^q = [u_1^q(k) - u_{max1}^q(k)][u_1^q(k) - u_{min1}^q(k)] \leq 0 \tag{3.26a}$$
$$h_2^q = [u_2^q(k) - u_{max2}^q(k)][u_2^q(k) - u_{min2}^q(k)] \leq 0 \tag{3.26b}$$

3.1.2 Objective Function

The objective function [13] that needs minimization, as showed in figure 3.2, is composed of five sub-objective functions regarding the fuel consumption and the passenger comfort, reaching desired speeds, the obstacle avoidance and the coupling of longitudinal and lateral speeds.
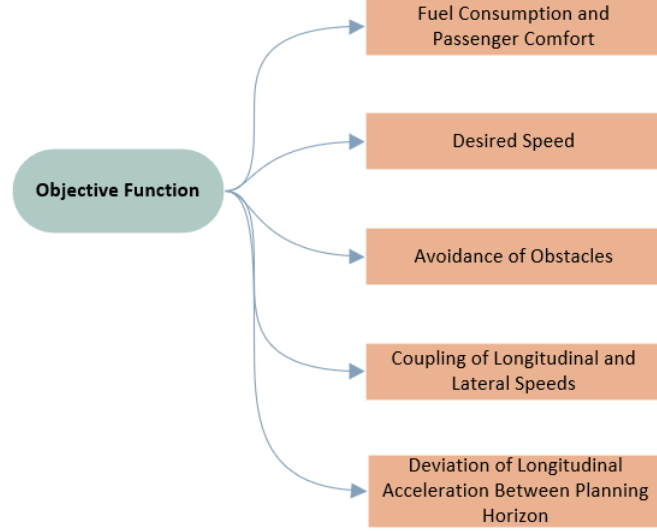
Figure 3.2: Objective function components

Fuel Consumption and Passenger Comfort

The first sub-objective function refers to fuel consumption and passenger comfort and it is given by equation 3.27. The fuel consumption is reduced only if the acceleration in the longitudinal direction become less severe. It has been proven that a quadratic term in each lateral $(u_2^q(k))^2$ and longitudinal $(u_1^q(k))^2$ direction is an excellent choice for minimizing fuel consumption, something that leads to a smoother acceleration, which benefits to passenger comfort [32].

$$(u_1^q(k))^2 + (u_2^q(k))^2 \tag{3.27}$$

Desired Speeds

The second sub-objective function refers to desired speeds and is given by equation 3.28. The vehicles have a pre-specified desired speed on both longitudinal and lateral directions and try to achieve this by minimizing the quadratic terms $(x_3^q(k) - u_{d1}^q(k))^2$ and $(x_4^q(k) - u_{d2}^q(k))^2$. The u_{di}^q with i=1,2, is the desired speed. In the work so far, the longitudinal desired speed has a positive value, while the lateral desired speed equals to zero. **In the current diploma thesis, it will be considered that the lateral desired speed has a non-zero value**. Of course, the vehicle's ability to advance depends on how close can drive to the longitudinal desired speed as well the traffic conditions around it.

$$(x_3^q(k) - u_{d1}^q(k))^2 + (x_4^q(k) - u_{d2}^q(k))^2 \tag{3.28}$$

Avoidance of Obstacles

The third sub-objective function refers to the avoidance of obstacles for safety reasons. An interaction zone is defined, and all vehicles which are inside this zone are considered as obstacles. The length of the interaction zone in both directions upstream and downstream is same and equal to the product of the longitudinal desired speed times the duration of the planning horizon. In the lane-based model, the constant time-gap (CTG) is used for keeping safe distances among the vehicles, using a linear function of the follower's speed multiplied by a coefficient, called time gap. For this work, an imaginary, and symmetric, in both directions longitudinal and lateral, ellipsoid hemisphere is considered around the obstacles. The ellipsoid's general form is shown in equation 3.29 and its role is to repel the vehicle to located inside the ellipsoid. Time gap parameters $(\omega_{x1}, \omega_{x2})$, the position and the speed of the ith obstacle among n obstacles in both directions are considered, respectively.

$$\left(\frac{x_1}{long}\right)^{P_1} + \left(\frac{x_2}{width}\right)^{P_2} \tag{3.29}$$

Longitudinal Direction

Begging with defining the length and the center of the ellipsoid in the longitudinal direction, the dimensions of both vehicles and obstacles should be covered by the ellipsoid. We define the augmented total length as $L_i = \mu_x(l_e + l_{oi})$, where l_e and l_{oi} are the length of the ego vehicle and the obstacle, respectively, and μ_x is a coefficient. Furthermore, is considered the following two-way function, which implements practically the CTG.

$$\text{Safety Gap} = \begin{cases} \omega_{x1}x_3^q, & \text{if the ego is behind the obstacle} \\ \omega_{x1}o_{i3}, & \text{if the ego is in front of the obstacle} \end{cases} \tag{3.30}$$

By positioning the center in the longitudinal direction, it is observed that, it depends on the speed difference of the ego vehicle and the obstacle. The center of the ellipsoid coincides with the center of the obstacle if the two vehicles has the same speed but, it is shifted longitudinally to cover the previous safety gap requirements, when the ego and the obstacle have different speeds. So, for the ellipsoid, the longitudinal axis is set and the longitudinal center is position as following respectively:

$$s_{d1} = L_i + \omega_{x1}x_3^q + \omega_{x1}o_{i3} \tag{3.31}$$

$$\delta_{oi} = o_{i1} - \frac{\omega_{x1}(x_3^q - o_{i3})}{2} \tag{3.32}$$

Lateral Direction

In the lateral direction, there is a problem only when the vehicles approaching each other laterally. In order to avoid the collision in the lateral direction, a safety gap towards this direction is set as it shown in the following equation:

$$\text{Safety Gap} = \begin{cases} \omega_{x2}|x_4^q - o_{i4}|, & \text{if the vehicles approach each other} \\ 0, & \text{otherwise} \end{cases} \tag{3.33}$$

In the lateral direction the midpoint of the ellipsis coincides with the center of the obstacle, however the positioning of the center in the lateral direction should be defined, accounting the mentioned features, as:

$$d_{d2} = W_i + \omega_{x2}[\tanh(o_{i2} - x_2^q)(x_4^q - o_{i4}) + \sqrt{[\tanh(o_{i2} - x_2^q)(x_4^q - o_{i4})]^2 + \epsilon_w}] \tag{3.34}$$

where $W_i = \mu_y(w_e + w_{oi})$ with the w_w and w_{oi} being the widths of ego vehicles and obstacles, ϵ_w being a small number, and μ_y being a coefficient -greater than 1- which ensures that the corner of the obstacle are covered.

The aim of the ellipsoid function is to penalize the approach among the vehicles, and to act as a crash avoidance term in the objective function. Moreover, the ellipsoid function should fulfill two more important requirements. Firstly, the form of the ellipsoid should covers the corners of the obstacle and be sufficient curvy in order to let the fast ego vehicles to slide around the slower obstacles in front of them. Parallel, the ellipsoid in 3-D plane should be steep in order its gradient be sufficient far the zero. Regarding this additional requirements the form of the ellipsoid is:

$$c_i(\boldsymbol{x}, \mathbf{o}_i) = \left\{ 1 - \tanh\left[\left(\frac{x_1^q - \delta_{o1}}{0.5d_1} \right)^{P_2} \left(\frac{x_2^q - o_{i2}}{0.5d_2} \right)^{P_2} \right] \right\} + \left\{ \frac{1}{\left[\left(\frac{x_1^q - \delta_{o1}}{0.25d_1} \right)^{P_3} + \left(\frac{x_2^q - o_{i2}}{0.25d_2} \right)^{P_4} \right]^{P_5} + 1} \right\} \tag{3.35}$$

The first term of the above equation fulfills the first additional criterion, while the second term fulfills the second additional criterion, respectively. Moreover, the ellipsis takes values in the interval of $[0, 1]$ and its general form for all obstacles is:

$$\sum_{i=1}^{n} [c_i(x, o_i)] \tag{3.36}$$

Coupling of Longitudinal and Lateral Speeds

The fourth sub-objective function refers to the coupling of longitudinal and lateral speeds and is given by equation 3.37. This equation is used in cases like low longitudinal speeds, where the model of equations of motion could lead to unrealistic and infeasible maneuvers, e.g moving only in the lateral direction.

$$f_c = \begin{cases} (\beta x_3(k)^q - x_4^q(k))^2, & x_4^q(k) > \beta x_3^q(k) \\ (\beta x_3^q(k) + x_4^q(k))^2, & x_4^q(k) < -\beta x_3^q(k) \\ 0 & otherwise \end{cases} \tag{3.37}$$

Deviation of Longitudinal Acceleration Between Planning Horizon

The fifth sub-objective function refers to the deviation of longitudinal acceleration between planning horizon and is given by equation 3.38. Each finite time planning horizon can start with any acceleration. This could results in discontinuities of the acceleration between the

planning horizons, due to the difference of the last applied and first applied acceleration in the longitudinal direction. These discontinuities can be minimized by penalizing the deviation between the starting acceleration $u_1^q(0)$ of a planning horizon and the final value of acceleration of the previous planning horizon $u_{1\text{prev}}^q(K-1)$.

$$f_d^q = \left[u_1^q(0) - u_{1\text{prev}}^q(K-1)\right]^2 \tag{3.38}$$

3.2   Lateral positioning strategy (LPS)

In this section, a lateral positioning strategy (LPS) is proposed for reaching the vehicle's desired lateral position according to its desired longitudinal speed, dependent on the penetration rate of each type of vehicles. This strategy aims to improve the traffic flow, by distributing the vehicles within the road according to their desired longitudinal speeds, under the premise "faster vehicles move farther left" and vice versa. In the research done so far by [13], the movement strategy in the lateral direction is using a desired lateral speed that is set to zero. The main idea of the new LPS is shown in figure 3.3.
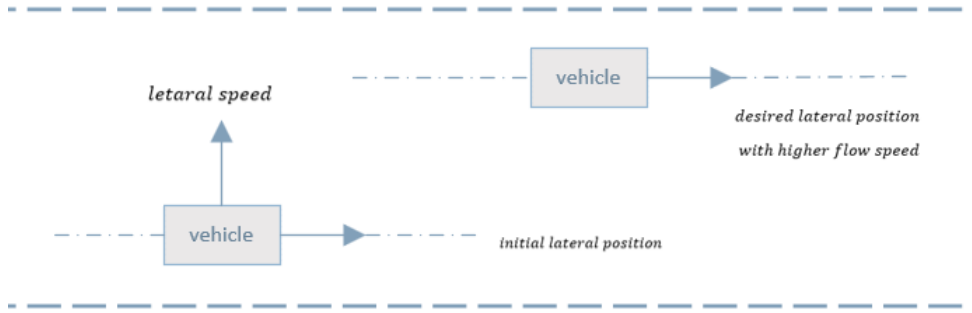
Figure 3.3: Basic idea

Continuous Distribution

The proposed methodology can be applied for both continuous and discrete distributions of the longitudinal desired speed. At this point the continuous distribution analysis will be presented. Firstly, the longitudinal desired speeds follow any distribution with a probability density function (f). The cumulative distribution function (CDF) of a random variable X, at point x, is the probability (in our case the percentage) that X will take a value less than or equal to that point and is given by the following equation:

$$F(x) = \int_{-\infty}^{x} f(t)dt \tag{3.39}$$

Considering a penetration rate (pr_i) of each type (i) of vehicles, we can calculate the desired position as a percentage ("new variable") of the available lateral space.

$$\text{"new variable"} = \sum_{i} pr_i F(x_{3des}^{q}) \tag{3.40}$$

where x_{3des}^{q} is the desired longitudinal speed of the qth vehicle that needs to be mapped into a lateral desired position. Formula 3.40 finds the percentage of the road in which a vehicle has a longitudinal desired speed greater than all the vehicles below it. By multiplying this percentage with the width of the road that a vehicle is allowed to move, the lateral desired position is found.

Implementation

Initially, a vehicle is placed randomly within the road and is allowed to move laterally within the range of $[\frac{W_v}{2}, W_r - \frac{W_v}{2}]$ resulting from the geometry shown in the figure 3.4, where W_v is the width of the vehicle, while the W_r is the width of the road.
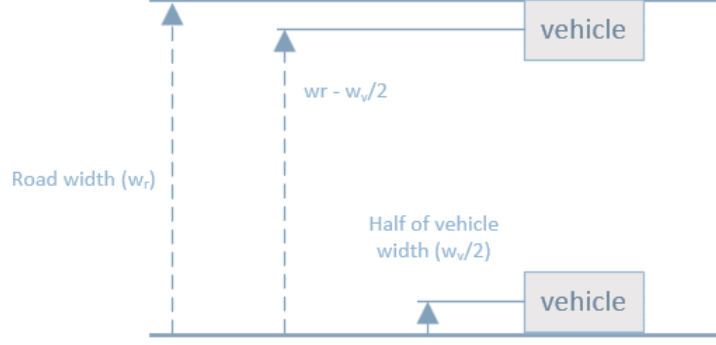
Figure 3.4: Lateral road boundaries

In our case, where two types of vehicles are used, trucks and regular cars, the penetration rate of each type is a and $1 - a$, respectively. The desired longitudinal speed ranges are overlapping and equal to $[v_1, v_2]$ and $[v_3, v_4]$ respectively. Also, the desired longitudinal speed is assigned with a uniform distribution and its CDF is given by the following equation:

$$F(x^q_{3des}) = \begin{cases} 0, & x^q_{3des} < v_i \\ \frac{x^q_{3des} - v_i}{v_j - v_i}, & v_i \leq x^q_{3des} < v_j \\ 1, & x^q_{3des} \geq v_j \end{cases} \quad (3.41)$$

where v_i and v_j with $i \neq j$ are the maximum and the minimum values of the desired longitudinal speed.

By combing the equation 3.40 with 3.41, equation 3.42 is obtained, that can map the longitudinal desired speed (x^q_{3des}) that is set to $[v_i, v_j]$ m/s to a lateral desired position (x^q_{2des}). Figure 3.5 illustrates the three calculation zones of this function.

$$x^q_{2des} = \begin{cases} a\frac{(x^q_{3des} - v_1)}{(v_2 - v_1)}(W_r - W_v) + \frac{W_v}{2}, & v_1 \leq x^q_{3des} < v_3 \\ (a\frac{(x^q_{3des} - v_1)}{(v_2 - v_1)} + (1 - a)\frac{(x^q_{3des} - v_3)}{(v_4 - v_3)})(W_r - W_v) + \frac{W_v}{2}, & v_3 \leq x^q_{3des} < v_2 \\ (a + (1 - a)\frac{(x^q_{3des} - v_3)}{(v_4 - v_3)})(W_r - W_v), & v_2 \leq x^q_{3des} \leq v_4 \end{cases} \quad (3.42)$$
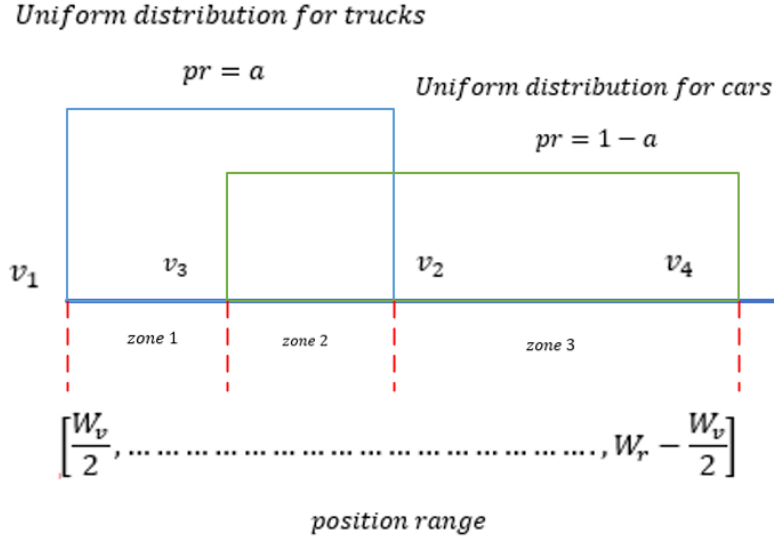
Figure 3.5: Graphical representation of equation 3.42

For our case, if a is equal to 0, i.e. the penetration rate for cars is equal to 1, and that means that only one type of a vehicle is used, then equation 3.42 is transformed into the following:

$$x_{2des}^q = \left(W_r - W_v\right)\left(\frac{x_{3des}^q - v_3}{v_4 - v_3}\right) + \frac{W_v}{2}, \quad \forall x_{3des}^q \in [v_3, v_4] \tag{3.43}$$

as $[v_3, v_4] \to [\frac{W_v}{2}, W_r - \frac{W_v}{2}]$.

Moreover, after the lateral desired position's calculation, a lateral desired speed that needs to be applied for the vehicle to lead it to its desired lateral position in a specified time (S) is derived by the equation of motion in the lateral direction, and is given by the following equation:

$$x_{4des}^q = \frac{x_{2des}^q - x_2^q(0)}{S} \tag{3.44}$$

Figure 3.6, illustrates this new strategy. The vehicle is placed in its initial position x_2^q and tries to reach its desired position x_{2des}^q in exactly S sec, by applying the constant lateral speed x_{4des}^q.
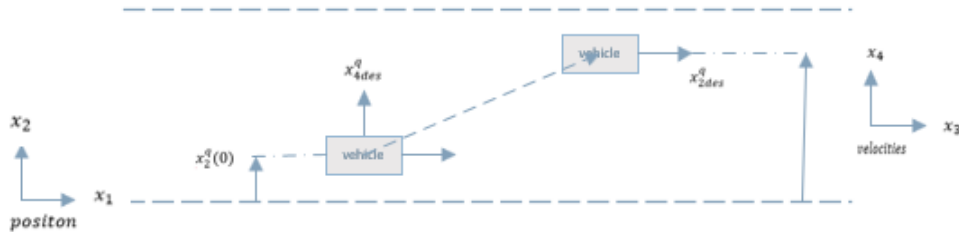
Figure 3.6: lateral positioning strategy

25

Example

Assuming two types of vehicles with penetration rate 10% and 90% respectively, we choose a vehicle with width $W_v = 1.6m$. A road with width $W_r = 10.2m$ is considered, and the lateral desired position range derives to be equal to [0.8,9.4]. The longitudinal speed range for the first type of vehicles is selected to be $[20, 27]$, while for the second is selected to be equal to $[23, 35]$. Also, the longitudinal desired speed is considered to be equal to 25 m/s. It is very clear, that the $x^q_{3des} = 25$ is in the second zone, so, the second branch of equation 3.42 is used, and the desired lateral position is:

$$x^q_{2des} = (0.1\frac{25 - 20}{27 - 20} + 0.9\frac{35 - 23}{35 - 23})(10.2 - 1.6) + 0.8 = 2.70 \tag{3.45}$$

This value of the lateral desired position is used in equation 3.44 in order to find the lateral desired speed, assuming that the achieved position and the time S are known.

Discrete Distribution

Up to this point, the LPS has been explained for continuous distributions, however this strategy can be implemented also with a discrete distributions of the longitudinal desired speeds i.e., $\{v_1, ..., v_n\}$ with respective probabilities $\{p_1, ..., p_n\}$. In order to calculate the lateral desired position, the allowable width of the road (W), i.e., $W = W_r - W_v$, needs to be spilt in corresponding parts $\{w_1, ..., w_n\}$, where $w_i = p_i \times W$ and hence $\sum_i w_i = W$. Therefore, each vehicle with longitudinal desired speed equal to v_i can be assigned in the w_i part of the road, in a homogeneously random way.

Example

We assume that we have a set with three different longitudinal desired speeds i.e. $\{25, 30, 35\}$ and some probabilities $\{0.2, 0.6, 0.2\}$ respectively. Then vehicles with longitudinal desired speed equal to 25 can be distributed randomly in the $0.2W$ part of the road, vehicles with speed equal to 30 can be distributed randomly in the $0.6W$ part of the road, and the rest vehicles to the rest of the road. Figure 3.7 shows the zones that the vehicles can be distributed according to their longitudinal desired speeds.
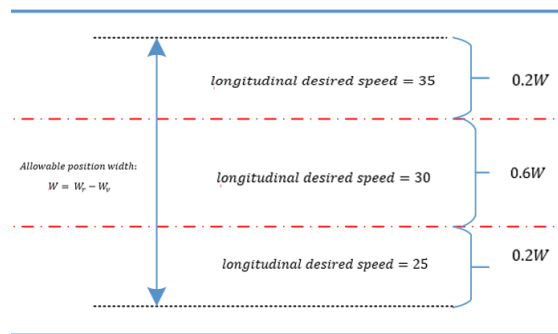

Figure 3.7: Graphical representation of the discrete distribution of the vehicles

3.3 Optimal Control Problem Formulation

According to section 2.5 the optimal path planning problem could be formulated as an optimal control problem (OCP). The objective function that needs minimization, can be written in the OCP form as:

$$
J = \sum_{k=0}^{K-1} \left\{ w_1(u_1^q(k))^2 + w_2(u_2^q(k))^2 + w_3(x_3^q(k) - u_{d1}^q(k))^2 + w_4(x_4^q(k) - x_{4des}^q(k))^2 \right.
$$
$$
\left. + w_5 \sum_{i=1}^{n} [c_i(\boldsymbol{x}, \mathbf{o}_i)] + w_6 f_c^q \right\} + w_7 f_d^q \tag{3.46}
$$

The difference from equation 2.1 is that equation 3.41 has not the term referring to the last step and it is independent from k. The equality constraints refer to the state equation 3.5, while the inequality constraints refers to equation 3.26.

The Hamiltonian function of this problem is defined as:

$$
\hat{H}[\boldsymbol{x}(k), \boldsymbol{u}(k), \boldsymbol{\lambda}(k), \boldsymbol{\mu}(k)] = \boldsymbol{\Phi}[\boldsymbol{x}(k), \boldsymbol{u}(k)] + \boldsymbol{\lambda}(k+1)^T \boldsymbol{f}[\boldsymbol{x}(k), \boldsymbol{u}(k)] + \boldsymbol{\mu}(k)^T \boldsymbol{h}[\boldsymbol{x}(k), \boldsymbol{u}(k)] \tag{3.47}
$$

Based on this, the necessary conditions of optimality 2.12 are satisfied. Finnaly, the boundary conditions are given by:

$$
\boldsymbol{x}(0) = \boldsymbol{x}_0 \tag{3.48}
$$

$$
\boldsymbol{\lambda}(K) = \mathbf{0} \tag{3.49}
$$

3.3.1 Solution

A Feasible Direction Algorithm (FDA) has been designed and applied for the solution of the OCP. The FDA for the discrete-time optimal control problems is practically an iterative algorithm, which attempts to find a local minimum in the mK-dimensional space of control variables. The OCP can be mapped in a Nonlinear Programming (NLP) problem in the reduced space of control variables, due to the explicit structure of the state equations, as well as, takes advantage of the necessary conditions of optimality. Moreover, FDA exploits the fact that $\boldsymbol{g}(k) = [\partial \boldsymbol{f}/\partial \boldsymbol{u}(k)]^T \boldsymbol{\lambda}(k+1) + \partial \boldsymbol{\Phi}/\partial \boldsymbol{u}(k)$ equals to reduced gradient. The multipliers of the inequality constraints that define bounds can be calculated by 2.12c. Figure 3.8 (a), displays the flow diagram of the FDA.

The FDA splits into four steps. Firstly, an initial guess for the control variables -initial trajectory- is required to begin the algorithm. Afterwards, the state variables, the Lagrange multipliers, the Kuhn-Tucker multipliers, and the reduced gradient are calculated in order to begin the first iteration. As next step, is the specification of a search descent direction. By using this search direction, the Line Optimization can begin to find the scalar step a, in order to compute the next state variables, the Lagrange multipliers, the Kuhn-Tucker multipliers, and
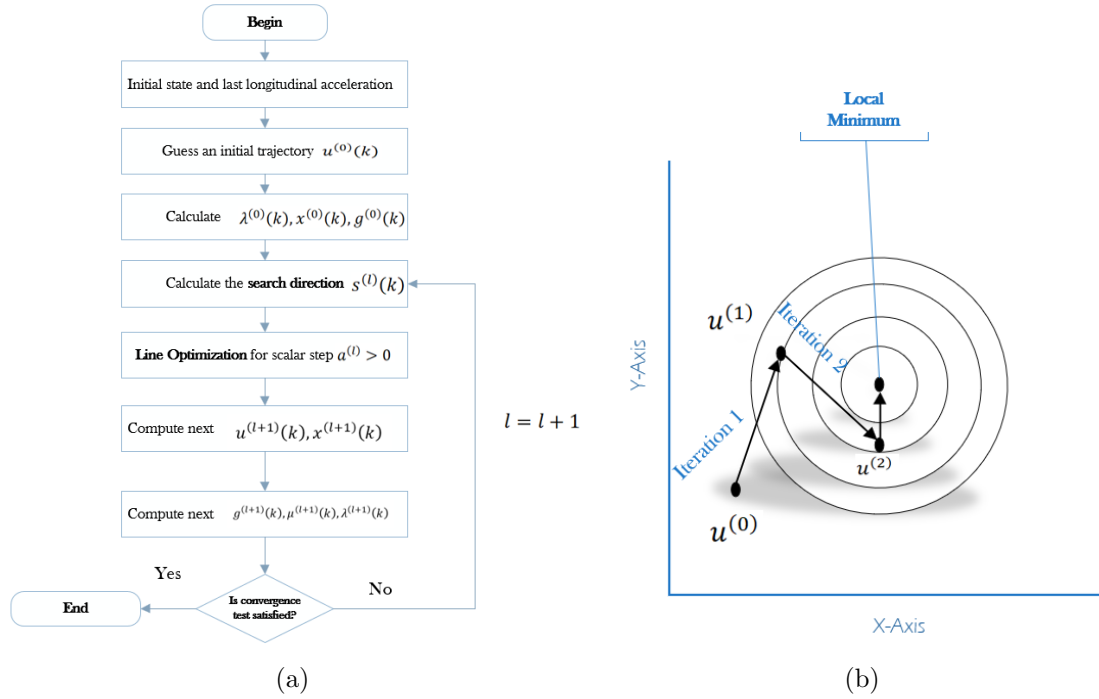
Figure 3.8: (a) Feasible Direction Algorithm (b) Schematic representation of algorithmic steps

the reduced gradient. Figure 3.8 (b), illustrates the schematic explanation of the algorithmic steps in the U-space, so far. Finally, through a convergence criterion is examined, if the reduced gradient converge to the zero. If it does then the optimal control problem satisfies all the necessary conditions of optimality and the problem is solved. If the criterion is not satisfied, then the improved control trajectory is the starting point of the next iteration, and the algorithm attempts to find a new search direction. It is remarkable that, a lot of algorithms can be used in order to find a search direction, like Polak-Ribiere, but for this problem the Fletcher-Reeves method was found the most efficient.

3.3.2 Model Predictive Control (MPC)

Model predictive control, also known as moving horizon control, is one of the most popular advanced control methods. MPC is based on a repeated real-time optimization of a mathematical system model The key point of MPC is to predict the future behavior of the system over a finite time horizon and to compute an optimal control input u. The optimal control input can be found through an optimization procedure, considering some given system constraints, and a cost function. The optimal control trajectory, can be calculated within a finite rolling horizon. Afterwards, the optimal input trajectory is applied to the system until the next sampling instant, at which the horizon is shifted and the whole procedure is repeated again [4].

In this problem, the event trigger MPC scheme is applied to all vehicles independently, while the FDA produces numerical solutions in real time for the optimization part. The time horizon for this problem is 8 sec, but the application period of the produced trajectories is 4 sec, because it is required to have smoother accelerations. Therefore, only the half of a trajectory is applied, while the rest is used as a initial value in the next iteration of FDA. These partial trajectories
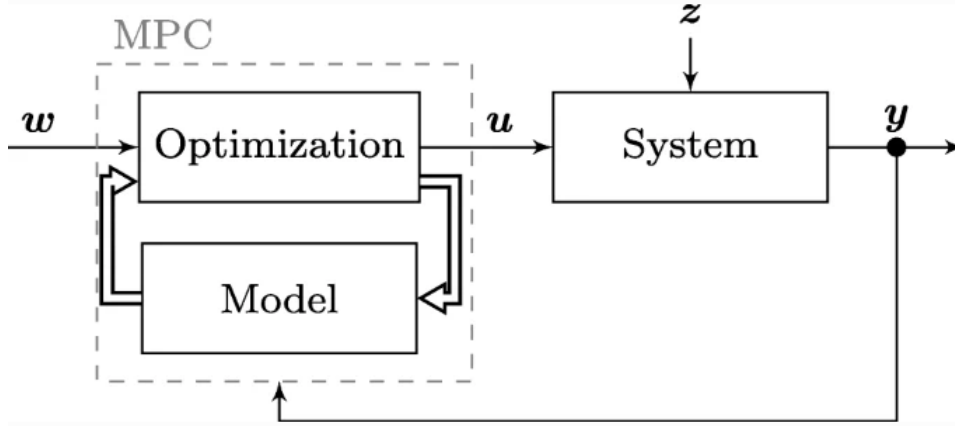
Figure 3.9: Model Predictive Control loop, Source: [4]

are supposed to cover the whole time horizon (8sec) by considering zero accelerations for the rest 4 sec.

However, there are some cases which the FDA is activated to produce new trajectories for the following reasons [33]:

- the vehicle has applied the last trajectory

- there is a substantial deviation in the path of the obstacles

- a new obstacle appears in the interaction zone

- a collision has predicted in the returning trajectory

Moreover, due to there is no guarantee to have a collision free trajectory, there have been some collisions detection and prevention in order to avoid this situations. The checks are about to detect a collision in both directions, lateral and longitudinal respectively. For the longitudinal direction, three conditions must be true at the same time in order to detect a crash.

- the initial position of the ego vehicle longitudinally, should be behind the obstacles center: $x_1^q(0) < o_{i1}^q(0)$

- overlap check of length and emergency time gap from front and rear sides: $(o_{i1}^q(k) - e_l^q/2 - o_{il}^q/2 - \omega_{1em}^q x_3^q(0)) < x_1^q(k) < (o_{i1}^q(k) + e_l^q/2 + o_{il}^q/2 + \omega_{1em}^q x_3^q(0))$, where $\omega_{1em} = 0.5\omega_1$

- lateral overlap checked of the width between the vehicle and the obstacle: $(o_{i2}^q(k) - e_w^q/2 - o_{w2}^q/2 - \epsilon) < x_2^q(k) < (o_{i2}^q(k) + e_w^q/2 + o_w^q/2 + \epsilon)$, where is a small safety margin

If a collision is detected, then the OCP is re-formulated with new upper limit in the state-dependent bound and tries to follow the obstacle. On the other hand, and similar to the longitudinal direction, a lateral collision can be detected when the following three conditions are parallel true:

- lateral alignment check: $(o_{i1}^q(k) - e_l^q/2 - o_{il}^q/2 - \epsilon < x_2^q(0) < (o_{i1}^q(k) + e_l^q/2 + o_{il}^q/2 + \epsilon$

- longitudinal overlap checked of the width between the vehicle and the obstacle: $(o_{i2}^q(k) - e_w^q/2 - o_{w2}^q/2 - \epsilon) < x_1^q(k) < (o_{i2}^q(k) + e_w^q/2 + o_w^q/2 + \epsilon)$, where is a small safety margin

- overlap lateral check: $(o_{i2}^q(k) - e_w^q/2 - o_{w2}^q/2 - \epsilon) < x_2^q(k) < (o_{i2}^q(k) + e_w^q/2 + o_w^q/2 + \epsilon)$, where is a small safety margin

If a collision is detected, then the OCP is re-formulated with new upper and lower limits in the state-dependent bounds, which restrict the movement laterally within ± 0.15 m of the initial lateral position.

Furthermore, it is required a longitudinal speed adaption due to two issues. Firstly, it might be a big difference between the longitudinal desired speed V_{des}^q and the initial longitudinal speed, something that may result in high acceleration values, and thus passenger discomfort. Secondly, due to high densities, the vehicles tend to move in groups with similar longitudinal speed, that are enough smaller than the desired one. In order to avoid this two issues, the desired longitudinal speed in the objective function should be adapted as it follows. According to 3.45, the adaptive longitudinal speed is limited between the real desired speed and the initial speed incremented by a positive value V_{incr1}^q. To address the second issue, the adaptive longitudinal speed is additionally limited by the actual average downstream longitudinal speed incremented by a positive value V_{incr2}, if the current density is above a threshold.

$$u_{d1}^q = \begin{cases} \min\{x_3^q(0) + V_{incr1}^q, V_{des}^q\}, & D_d \leq D_{bar} \\ \min\{x_3^q(0) + V_{incr1}^q, D_u + V_{incr2}, V_{des}^q\} & \text{otherwise} \end{cases} \tag{3.50}$$

CHAPTER 4

SIMULATION SET-UP

Chapter 4 presents the simulation environment and the two main scenarios that used for the validation and the effectiveness on the proposed strategy. Section 4.1 provides information about the custom made extension that is used for the simulation environment. Section 4.2.1 describes the first scenario, that uses regular passenger vehicles with different dimensions, while section 4.2.2 presents, the second scenario, that uses both trucks and vehicles in different dimensions. In both scenarios, two cases are examined, the Base Case (BC) and the LPS case.

4.1 Simulation Environment

4.1.1 TrafficFluid-Sim

The traffic simulations took place in a lane-free environment, via a custom made extension called TrafficFluid-Sim [19] for the Simulation of Urban MObility (SUMO) simulator [20]. TrafficFluid-Sim is a microscopic simulator which aims to V2V and/or V2I communication. The development of this extension was based on the two principles of the novel paradigm called TrafficFluid. Firstly, the environment where a vehicle can move has no lanes, and hence the vehicles can be located any where in the road. Secondly, the vehicles use the nudging effect to other vehicles which are located in their interaction zone. The purpose of this simulator is to provide the ability to use various -custom made- movement strategies for a lane-free environment, including the nudging effect. In lane-based SUMO, vehicle strategies are often organized using two types of models: a "Car-Following" model and a "Lane-Changing" model. These models control the longitudinal speed and lane placement appropriately. The use of lane-free vehicle controllers with this type of architecture is obviously inappropriate.

Therefore, the extension provides a dynamic library for lane-free vehicles movement control, as well as, some functionalities between FDA and SUMO, like, the option of setting the lateral position of the vehicles and their desired speed in the longitudinal direction, via an application programming interface (API). Moreover, the dynamic library, allows coding development in C/C++, which provides the ability of creating a coding structure which contains both a initialization and finalization functions. The user can develop control strategies through programming, and test them via the SUMO. At the end, the API offers a wide range of information

31

regarding: the properties of the vehicle, like width or length, or the actual status such as, the position or the speed, and their own control through their unique ID. Also, the API provides information about the road, where the vehicles are operating, like the length, and the width.
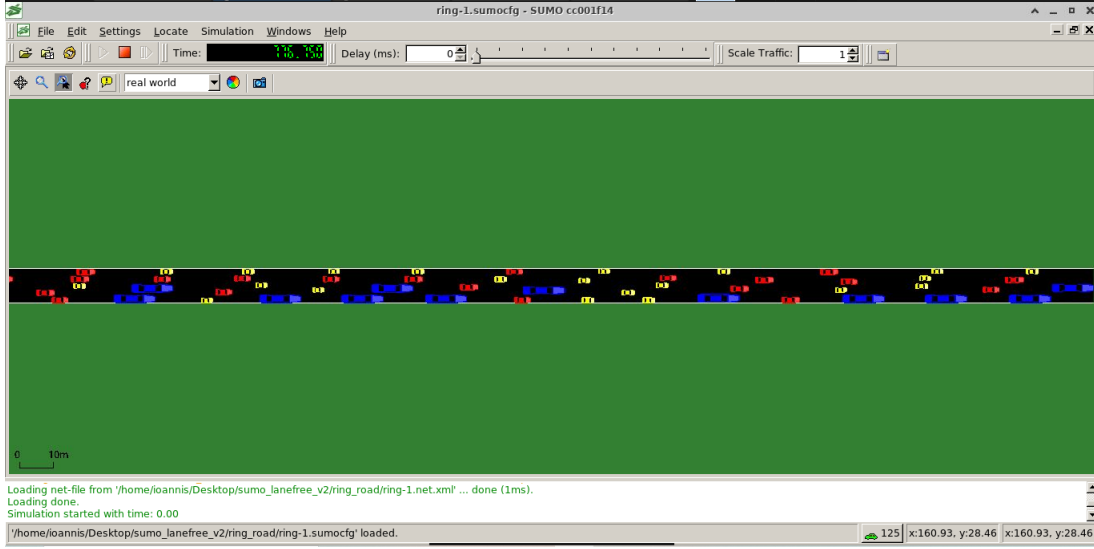
Figure 4.1: Simulation Environment

4.2 Scenarios

Two traffic scenarios have been tested, with different parameters. For each scenario, two simulations have been run, one without the LPS (called base case), and one simulation applying the proposed strategy.

4.2.1 Scenario 1

In this scenario, only regular passenger vehicles with different dimensions are used in a lane-free unfolded ring road, which has length and width equal to 1 km and 10.2 m respectively. Table 4.1 represents the 8 classes of vehicles based on their the dimensions.

Class	I	II	III	VI	V	VI	VII	VIII
Length (m)	3.2	3.4	3.9	4.25	4.55	4.6	5.15	5.2
Width (m)	1.6	1.7	1.7	1.8	1.82	1.77	1.84	1.88

Table 4.1: Regular passenger vehicle dimensions

For the vehicles placement, the road is separated into four pseudo-lanes laterally and in $n/4$ sections longitudinally, where n is the number of vehicles. The four pseudo-lanes with the $n/4$ sections develop n exactly cells in which the vehicles are placed randomly. Figure 4.2 illustrates the cells where the vehicles are placed for $n = 8$.
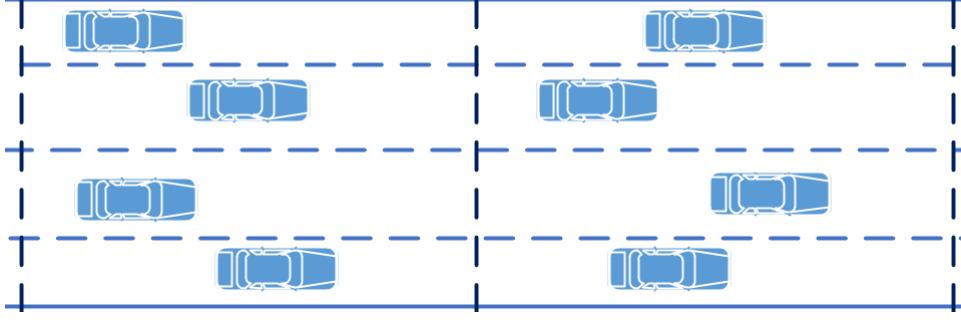
Figure 4.2: Initial placement for regular passenger vehicles

The longitudinal desired speed is set in the range of $[25, 35]$ m/s, and is assigned randomly to each vehicle using a uniform distribution.

Table 4.2 summarizes all the parameters referring to the objective function (3.41), safety parameters (3.30), crash avoidance and detection (3.45) etc. The parameters have been selected after various simulations. The big value of $w_5 = 7.0$ refers to the weight of the ellipsoid and its role is to enforce the obstacle avoidance. The simulation duration is half an hour, while the flow values are recorded for the last 10 min. Moreover, various densities of vehicles starting from 25 and end up 350 in different numbers of replications have been used.

w_1	w_2	w_3	w_4	w_5	w_6	w_7	ω_1	ω_2	ϵ_1	p_1	p_1	p_2	p_3	p_4	β	$D_{bar}(veh/km)$	T (ms)	K
0.01	0.01	0.03	different values	7.0	0.01	0.2	0.35	0.5	0.1	6	2	2	2	2	0.03	150	250	32

Table 4.2: Parameters set up for scenarios 1 and 2

Base Case (BC)

In the research done so far by [13], the lateral desired speed was set equal to zero. This case is considered to be the Base Case (BC) for comparison reasons. In the BC the weight parameter for the lateral desired speed is equal to 0.01. The weight in this case is small because it is less important to achieve the lateral position, compared to the goal to achieve the desired longitudinal speed.

LPS Case

The lateral desired position is selected based on the distribution of the longitudinal desired speed. With regard to LPS, the lateral desired speed is applied to each vehicles in real-time to reach their desired lateral position. Furthermore, in order to asses the impact of the weight w_4, three different values ($w_4 = 1, 3, 5$) for a specific density, in this case at 150 veh/km, have been used. After the vehicles have been placed randomly within the road, they must try to reach their desired longitudinal speed, and their lateral desired position. They start from zero speed and gradually speed up until the goal is satisfied. Simultaneously, the vehicles try to avoid any collisions with obstacles within their interaction zone.

4.2.2   Scenario 2

In this scenario both trucks and regular vehicles with different dimensions are considered, while the same road parameters are used. The penetration rate for trucks is 10%, while for cars is the rest (90%). Table 4.3 represents the dimensions of the vehicles, which are divided into 5 classes. The first class describes the trucks (blue), the second and the third describes the big size cars (red), while the two last class describes the small ones (yellow).

Class	I	II	III	VI	V
Length (m)	12.5	5.5	5.0	3.5	3.8
Width (m)	2.5	1.90	1.80	1.60	1.70

Table 4.3: Trucks and regular passenger vehicle dimensions

As in the scenario 1, the hypothetical lanes and cells in the road are used again for the initial placement of the vehicles. However, in this scenario, the trucks are placed randomly in the first pseudo-lane, while the rest of the vehicles are placed randomly in the other three. Figure 4.3 represents the initial placement of the vehicles, again for $n = 8$.
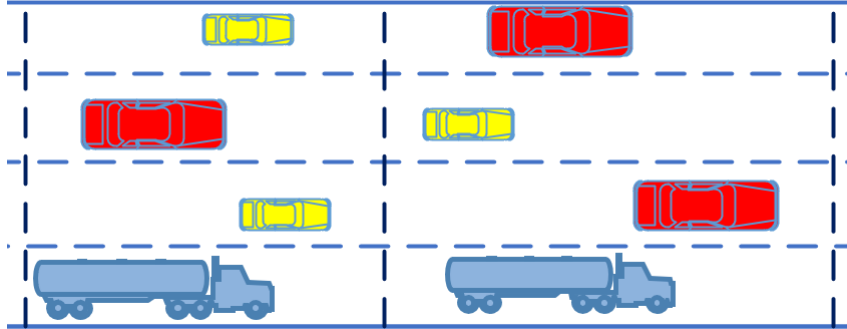

Figure 4.3: Initial placement for trucks and regular passenger vehicles

The speed range for the trucks is different from the regular vehicles and equal to $[20, 27]$ m/s, while the speed range for the rest of the vehicles is equal to $[23, 35]$ m/s. The speed ranges in this scenario are overlapping, while the longitudinal desired speeds are set to each vehicle according to the uniform distribution. The speed range separation has been done due to the different truck's capabilities in comparison to the regular vehicles. Moreover, a different value of truck deceleration is used due to the hypothesis that trucks have different deceleration capabilities, when they carry cargo. In that case, the deceleration decreases. So, the deceleration is picked to be equal to -4 m/s^2.

Table 4.2 for scenario 1 summarizes all the parameters referring to the objective function etc, also for this scenario. The simulation duration is again half an hour, and the flows achieved are recorded for the last 10 min. In addition, various densities of vehicles starting from 110 and end up 240 in different numbers of replications have been used.

Base Case (BC)

The BC in this scenario is basically the same as in scenario 1, simply adding trucks. The lateral desired speed is set again equal to zero, and the weight parameter $w_4 = 0.01$, due to the fact that also in this case, the goal of reaching the lateral desired position is less important than reaching the lateral desired speed.

LPS Case

Also, the LPS case for this scenario is basically the same as in scenario 1. Beside adding trucks, smaller weight values for the lateral speeds have been used i.e. $w_4 = 0.01, 0.1, 1$, for a density at 130 veh/km, as the presence of the trucks increases the possibility of collisions.

CHAPTER 5

RESULTS

Chapter 5 presents the statistical evaluation, as well as, the results (tables, diagrams) of the scenarios that were described in Chapter 4. Section 5.1 describes the statistical tools such as Average-MAE which try to give a mathematical assessment of the applicable lateral desired position. On the other hand, section 5.2 gives the traffic and the vehicle level results for two scenarios.

5.1 Statistical Evaluation

The evaluation of the various scenarios is achieved by the calculation of several quantities, such as, the average flow and some statistical quantities of the error in the lateral direction. Statistical evaluation helps to confirm weather the proposed methodology is efficient or not.

Calculated quantities

Flow (veh/h)

Flow (q) is the number of vehicles passing a reference point per unit time and it is calculated over the last 10 min of half an hour simulation, to make sure that the readings are taken after the traffic reaches some steady state.

Metrics

The average Mean Absolute Error (Average MAE) in the lateral position is calculated between the actual and desired position for all time steps, and for all vehicles, using the formula below:

$$\text{Average MAE} = \frac{\sum_{q=1}^{n} \left[\frac{\sum_{i=1}^{\text{tnss}} |x_2^q(i) - x_{2des}^q(i)|}{tnss} \right]}{n} \tag{5.1}$$

where $tnss$ is the total number of simulation steps. The standard deviation of MAE (stdvMAE) is calculated using the following formula:

$$\text{stdvMAE} = \sqrt{\frac{\sum_{q=1}^{n}\left[\frac{\sum_{i=1}^{\text{tnss}}[|x_2^q(i)-x_{2des}^q(i)|-AverageMAE]^2}{tnss}\right]}{n}} \quad (5.2)$$

The average Mean Error (Average-ME) in the lateral position is calculated for all time steps and for all vehicles and it is expressed by the following formula:

$$\text{Average-ME} = \frac{\sum_{q=1}^{n}\left[\frac{\sum_{i=1}^{\text{tnss}} x_2^q(i)-x_{2des}^q(i)}{tnss}\right]}{n} \quad (5.3)$$

5.2 Traffic and Vehicle Level Results

Traffic level simulations are run in a lane-free setup using a custom-made API called as TrafficFluid-Sim, developed within Simulation of Urban Mobility (SUMO) simulator as described in section 4.1. To test the proposed scheme, the approach is applied independently to all the vehicles driving on on ring-road of length 1 km and width 10.2 m, which is unfolded as discussed in Chapter 4. To evaluate the scenarios, the average flows achieved during the last ten minutes of half-hour simulations are measured.

5.2.1 Results for Scenario 1

First, an investigation has been done using three different values for the weight w_4 to asses the impact on the flow and on the metrics, using a density at 150 (veh/km). Tables 5.1 - 5.3 summarize the results of the flows and of the metrics.

Density: 150 (veh/km)	BC		LPS with weight: 1	
Replications	Flow (veh/km)		Average MAE (m)	Stdv MAE (m)
1	14745	15732	1.432	2.627
2	14811	15409	1.395	2.688
3	14965	15518	1.389	2.519
4	15051	15494	1.543	2.694
5	14816	15543	1.507	3.065
Average	14878	15539	1.453	2.719
stdv	112.71	106.42		
Flow improvement		4.45%		

Table 5.1: Flows for the BC, flows and metrics for LPS (weight equal to 1) and density of 150 veh/km

Density: 150 (veh/km)	BC		LPS with weight: 3	
Replications	Flow (veh/km)		Average MAE (m)	Stdv MAE (m)
1	14745	15655	1.085	2.235
2	14811	15481	1.013	2.192
3	14965	15688	1.045	1.911
4	15051	15644	1.078	2.362
5	14816	15442	1.068	1.929
Average	14878	15582	1.058	2.126
stdv	112.71	100.21		
Flow improvement		4.73%		

Table 5.2: Flows for the BC, flows and metrics for LPS (weight equal to 3) and density of 150 veh/km

Density: 150 (veh/km)	BC		LPS with weight: 5	
Replications	Flow (veh/km)		Average MAE (m)	Stdv MAE (m)
1	14745	15722	1.023	2.217
2	14811	15379	0.896	2.193
3	14965	15826	0.893	2.097
4	15051	15597	0.960	2.275
5	14816	15504	0.929	2.078
Average	14878	15606	0.940	2.172
stdv	112.71	157.40		
Flow improvement		4.89%		

Table 5.3: Flows for the BC, flows and metrics for LPS (weight equal to 5) and density of 150 veh/km

Figures 5.1 and 5.2 give a more comprehensive view of the above tabulated results. As it was expected, as the weight is increasing the Average-MAE decreases. This is shown in figure 5.2 (a), which illustrates the average-MAE for the 5 replications over the three different weights. Figure 5.2 (b) illustrates the standard deviation for the three different weights. In all cases, the flow achieved with the new LPS is improved. The bars in all figures reflect the range of values over the 5 different replications. Given that the stdv-MAE is smallest for the weight equal to 3 and this gives similar flow improvement, compared to the weight equal to 5, this value ($w_4 = 3$) was selected for further investigation of this scenario.
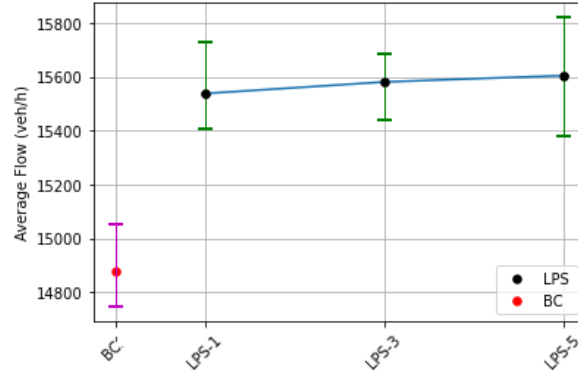
Figure 5.1: Average flow for the BC and the LPS for three different values of the weight


(a)	(b)
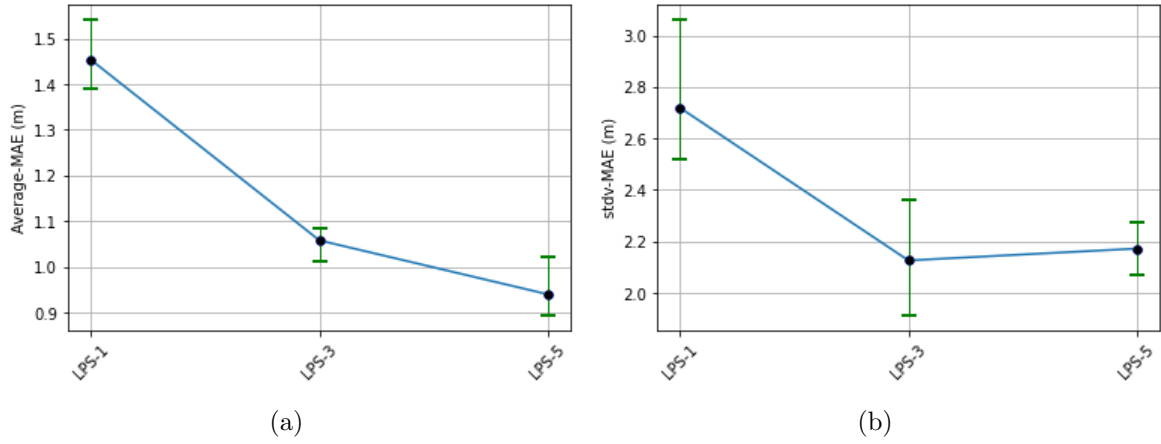
Figure 5.2: (a) Average-MAE for three different values of the weight (b) stdv-MAE for three different values of the weight

The average flows for both BC ad LPS cases of this scenario, were measured during the last ten minutes of a half-hour simulation for different densities and 5 replications per density. Figure 5.3 displays the fundamental diagram i.e. the measured average flows against the various densities for both, BC and LPS. The bars reflect the range of values over the 5 different replications. Note that the proposed strategy has virtually no effect for very low and overcritical densities. For the very low densities there is no improvement of the flow, since, the vehicles have the appropriate space to overtake the slower vehicles and reach their desired longitudinal speed.

The critical density is reached at 200 (veh/km). For densities below and near to the critical, the LPS helps the vehicles to move in their speed zone, avoiding the slow ones. For densities beyond the critical, there is little space for maneuvers, hence the new strategy does not offer any visible advantage. Finally, for very high densities, a flow decrease is observed when using the proposed strategy. This is due to a high number of emergency situations, i.e. avoiding collision, occurring in higher densities, probably due to the additional lateral movements caused by the new sub-objective. Thus, one may consider applying proposed strategy only around the critical density, where improvements are pronounced.
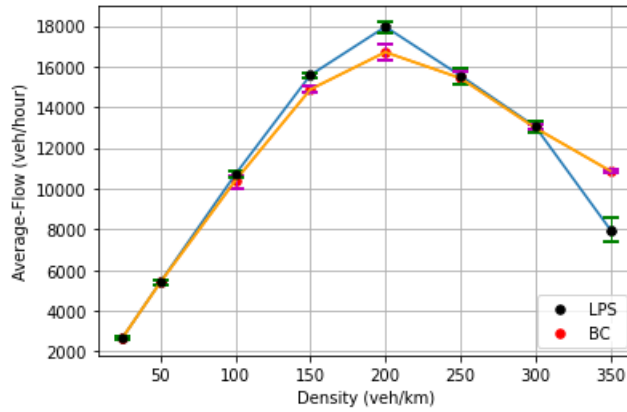
Figure 5.3: Fundamental Diagram

Table 5.4 presents the improvement on average of each flow that occurs from the fundamental diagram. The best improvement (7.47%) is achieved at the critical density, while the worst (-26.60%) at the 350 veh/km.

Density (veh/km)	25	50	100	150	200	250	300	350
Flow Improvement	-0.04%	0.27%	3.65%	4.73%	7.47%	0.81%	0.47%	-26.60%

Table 5.4: Flow Improvement over the BC per density

The Average-ME shows the deviation between the lateral desired position and the achieved position of the vehicles. Basically, Average-ME shows if the vehicles are above or below their lateral desired position. According to figure 5.4, which illustrates the distribution of the Average-ME (for the average and the range of values achieved over 5 replications), the majority of the vehicles are below their lateral desired position, while τhe bars reflect the range of values over the 5 different replications.
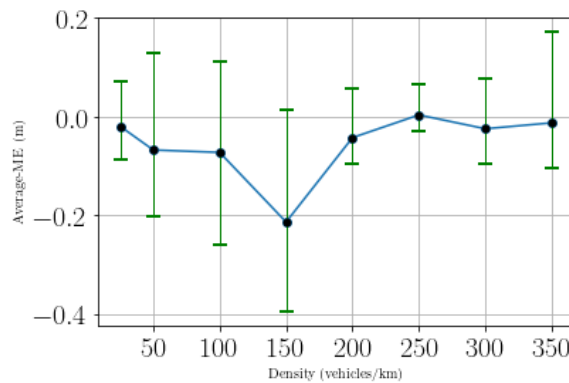

Figure 5.4: Average-ME for weight equal to 3 per density

Figures 5.5 - 5.7 illustrate some typical plots for the lateral desired speed for the three different penalties. The green dashed line represents the target lateral position, while the red one, represents the achieved position of the vehicle at each time step. It is observed that while the penalty term is increased the deviation between the desired lateral position and achieved position is getting smaller.
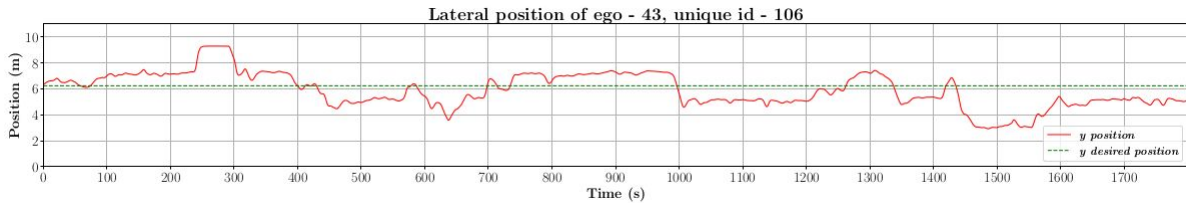

Figure 5.5: Lateral desired position behavior for a vehicle with weight equal to 1
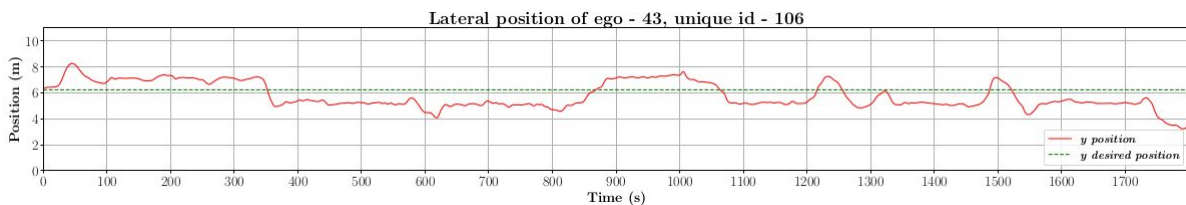

Figure 5.6: Lateral desired position behavior for a vehicle with weight equal to 3
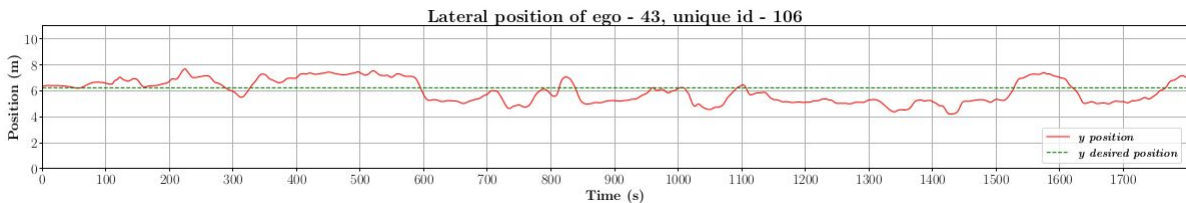
Figure 5.7: Lateral desired position behavior for a vehicle with weight equal to 5

Figures 5.8 and 5.9 display the longitudinal desired speed for a low and a high density respectively. For low densities the longitudinal desired speed converges quickly to the desired due to the fact that there is enough space for vehicle's movement. This is why, a vehicle in the density of 25 veh/km presents its convergence around 100 sec at a desired longitudinal speed equal to 30 m/s (see figure 5.8). On the other hand, in densities especially over critical, the longitudinal desired speed is not achieved because of the reason that there is no free space enough for the vehicle's movement to achieve the desired longitudinal speed, but it converges to a speed below the desired value. Therefor a vehicle in density of 300 veh/km, can not reach its desired speed, but it converges after 500 sec to a speed around 11 m/s (see figure 5.9).

Furthermore, there are cases where a vehicle has a constant deviation between its lateral desired position and its achieved position. Figure 5.10 displays this case, and the constant deviation is shown in the following time slot approximately: [300, 570]. The simulation has shown that, this happens due to there is another vehicle next to it, and it does not let the ego to reach its target position laterally.
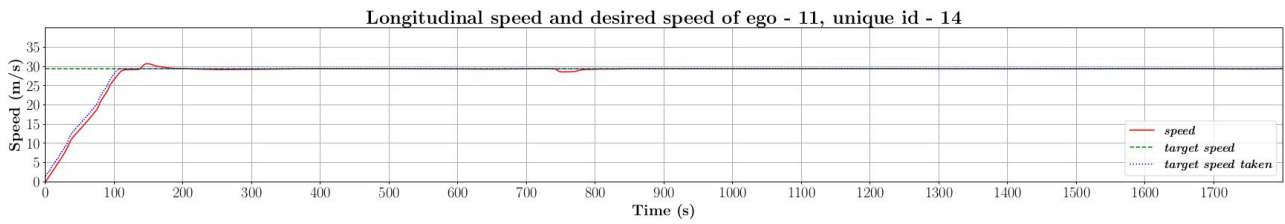
Figure 5.8: Longitudinal speed representation for a in density of 25 with weight equal to 3
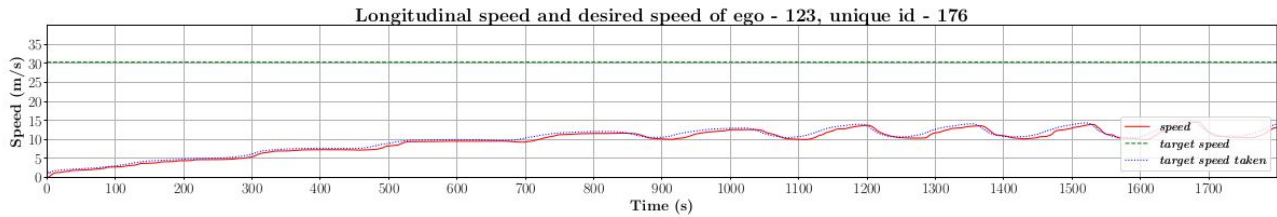

Figure 5.9: Longitudinal speed representation for a density of 300 with weight equal to 3
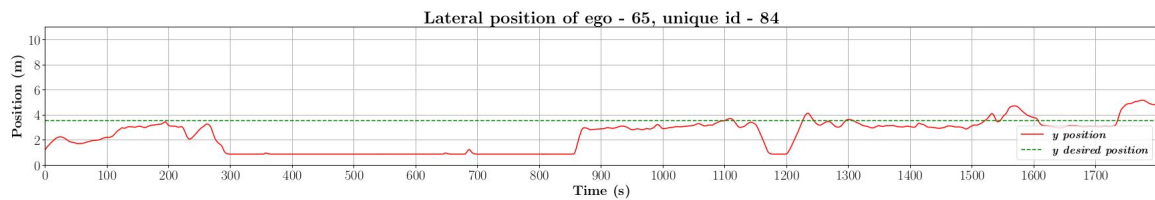

Figure 5.10: Lateral desired position behavior for a vehicle with weight equal to 3

From figure 5.10, it can be observed that between 300 s and 850 s, the vehicle stays on the right side of the desired lateral position. As a result of this, the desired lateral speed during the same period is greater than the actual lateral speed. The vice-versa happens during the brief time where the vehicle goes left of the desired lateral position. The behaviour is in accordance with equation 3.44, which generate both positive and negative values according to the requirement and this further observed from figure 5.11.
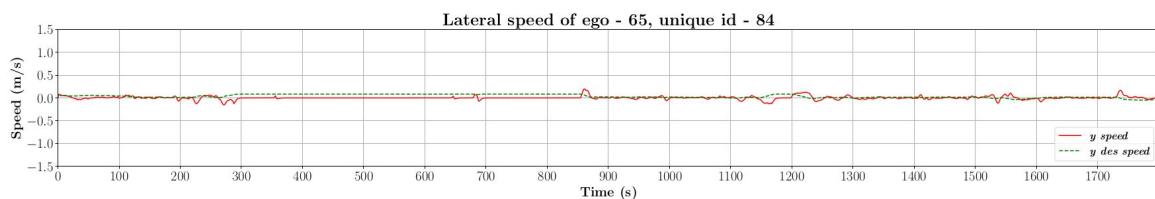

Figure 5.11: Lateral desired speed behavior for a vehicle with weight equal to 3

42

5.2.2 Results for Scenario 2

Also for this scenario, three different values for the weight are used to investigate the impact on the flow and metrics, using a density at 130 (veh/km). Tables 5.5 - 5.7 summarize the results of the flows and of the metrics.

Density: 130 (veh/km)	BC		LPS with weight: 0.01	
Replications	Flow (veh/km)		Average MAE (m)	Stdv MAE (m)
1	11691	12009	3.262	2.367
2	12088	11853	3.665	2.315
3	11536	11878	3.600	3.064
4	12373	12159	3.367	3.006
5	12002	11934	3.367	3.200
Average	11938	11967	3.294	2.790
stdv	296.12	110.12		
Flow improvement		0.24%		

Table 5.5: Flows for the BC, flows and metrics for LPS (weight equal to 0.01) and density of 130 veh/km

Density: 130 (veh/km)	BC		LPS with weight: 0.1	
Replications	Flow (veh/km)		Average MAE (m)	Stdv MAE (m)
1	11691	12195	2.578	2.494
2	12088	12142	3.017	2.081
3	11536	11670	2.241	2.995
4	12373	12638	2.534	2.323
5	12002	12174	2.657	3.080
Average	11938	12164	2.605	2.605
stdv	296.12	306.68		
Flow improvement		1.89%		

Table 5.6: Flows for the BC, flows and metrics for LPS (weight equal to 0.1) and density of 130 veh/km

Density: 130 (veh/km)	BC		LPS with weight: 1	
Replications	Flow (veh/km)		Average MAE (m)	Stdv MAE (m)
1	1 11691	12205	1.630	2.462
2	12088	12469	1.661	1.975
3	11536	12228	1.528	1.838
4	12373	12883	1.611	1.504
5	12002	12429	1.571	1.511
Average	11938	12443	1.600	1.858
stdv	296.12	243.86		
Flow improvement		4.23%		

Table 5.7: Flows for the BC, flows and metrics for LPS (weight equal to 1) and density of 130 veh/km

Also for this scenario, figures 5.12 and 5.13 give a more comprehensive representation of the tabulated values. As was expected, when the weight is increasing, the Average-MAE decreases. This is shown in figure 5.13 (a), which illustrates the average-MAE for the 5 replications over the three different weights we used. Figure 5.13 (b) illustrates the standard deviation for the three different weights. In all cases, the flow achieved with the new LPS is improved. The improvement for this scenario is more significant than in the previous scenario. The bars in all figures reflect again the range of values over the 5 different replications. Given that the stdv-MAE is smallest for the weight equal to 1 and this gives the best flow improvement, compared to other weights, this value ($w_4 = 1$) was selected, for further investigation of this scenario.
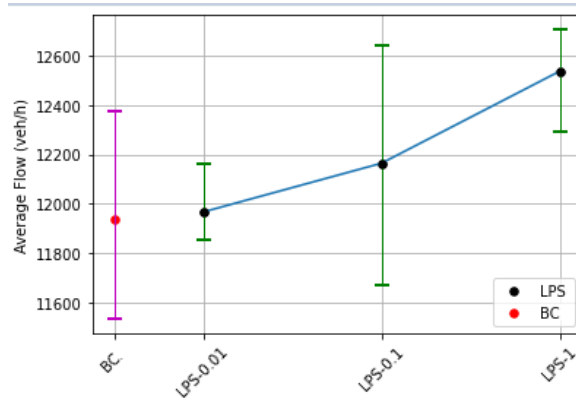

Figure 5.12: Average flow for the BC and the LPS for three different values of the weight
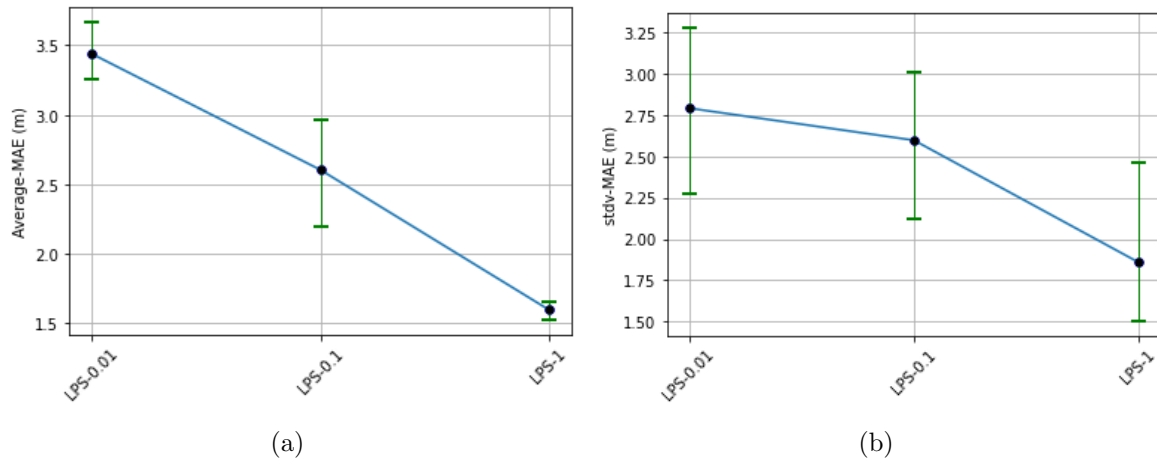
Figure 5.13: (a) Average-MAE for three different values of the weight (b) stdv-MAE for three different values of the weight

Similar to the previous scenario, the average flow values for both BC and LPS cases were measured based on 5 replications per density, during the last ten minutes of a half-hour simulation for different densities. Figure 5.14 shows the fundamental diagram i.e. the measured average flows over the the various densities for both BC and LPS. The bars, also in this case, reflect the range of values for the 5 different replications. Note that the proposed LPS results always in a flow improvement per density. For densities below the critical the improvement in the flow is small, but significant, because there is enough space for overtaking slower vehicles.

The critical density is obtained at 180 (veh/km). The new strategy achieved the goal in every density. It is observed that in every density there is an improvement in the traffic flow. For high and very high densities, a significant flow increase is observed when using the proposed strategy. This is due to the appropriate distribution of the vehicles laterally in the road. Another reason is that in BC, the big trucks may occupy more than half of the road especially when a truck overtakes another truck. Taking into account that the longitudinal speeds for the trucks are smaller than the car's speeds, all the upstream vehicles slow down significantly. On the contrary, during the simulations with LPS, it was observed that the trucks remained at the bottom of the road, for the majority of the simulation time, allowing higher traffic flows. Hence, one may consider that by applying this new strategy for different penetration rates, an improvement is observed over a wide range of densities.
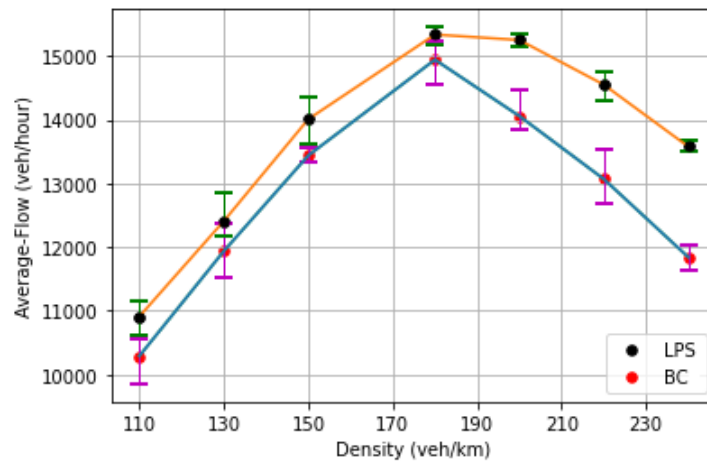
Figure 5.14: Fundamental Diagram

Table 5.8 presents the improvement on average of each flow that occurs from the fundamental diagram. The best improvement (15%) is achieved at density equal to 240 veh/km, while the worst (2.64%) at the critical density 180 veh/km.

Density (veh/km)	110	130	150	180	200	220	240
Flow Improvement	6.03%	4.23%	4.46%	2.64%	8.92%	11.35%	15%

Table 5.8: Flow Improvement over the BC per density

In this scenario, and according to figure 5.15, which illustrates the distribution of the Average-ME (for the average and the range of values achieved over 5 different replications), there are vehicles observed in both below and above their lateral desired position. Furthermore, the bars reflect the range of values over the 5 different replications.
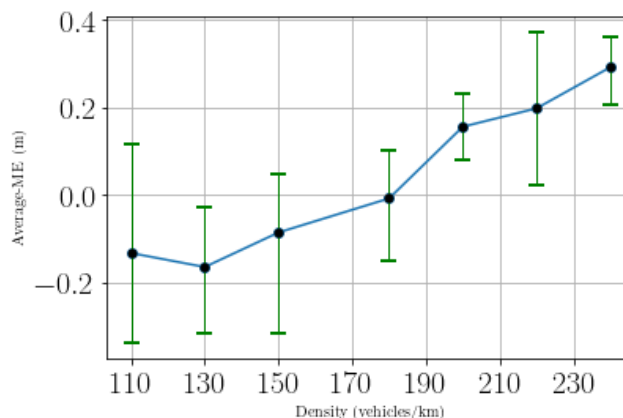

Figure 5.15: Average-ME for weight equal to 1 per density

Figures 5.16 - 5.18 illustrate some typical plots for the lateral desired position for the three penalties over the time. The green dashed line represents the lateral desired position, while the

red, represents the actual lateral position. It is obvious, that while the weight for the lateral desired speed is increased, then the vehicle is forced to reach and to remain to its target lateral position. There are time slots in which the target position is achieved exactly, but sometimes there is a fluctuation around the target position, because the vehicle maneuvers to avoid a collision or overtake a slower vehicle.
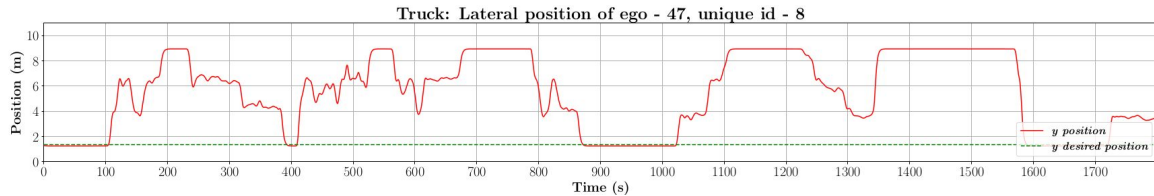

Figure 5.16: Lateral desired position behavior for a vehicle with weight equal to 0.01
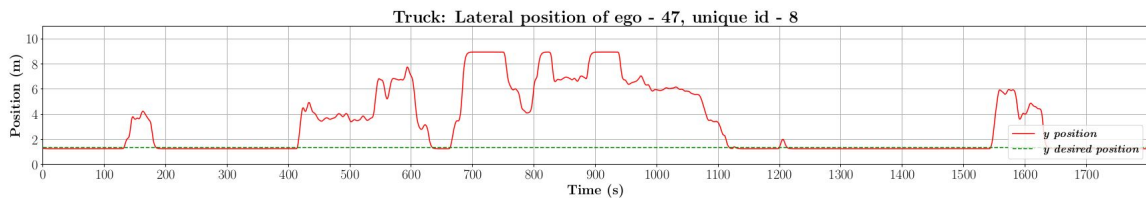
Figure 5.17: Lateral desired position behavior for a vehicle with weight equal to 0.1
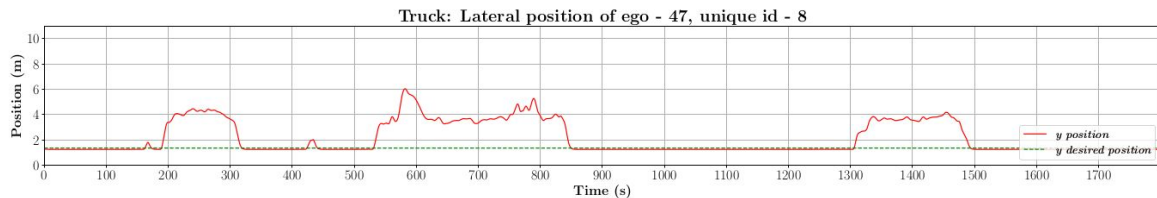

Figure 5.18: Lateral desired position behavior for a vehicle with weight equal to 1

Again in this scenario, it is confirmed that in lower densities vehicles are converging to their longitudinal desired speed quickly, while in higher densities they are not. Therefore, a vehicle in density of 130 veh/km converge to its desired longitudinal speed which is approximately 27 m/s, in around 100 s and this is given in figure 5.19. On the other hand, for over critical densities, the desired longitudinal speed is not achieved. A vehicle in density of 240 veh/km, can not reach its target speed, but it converges after 800 sec to a speed around 15m/s (see figure 5.20).

Also in this scenario, there are cases where a vehicle has a constant deviation between its lateral desired position and its achieved position. Figure 5.21 displays this case, and the constant deviation is shown in the following time slots approximately: [50, 680], [920, 1020] and [1220, 1390] in seconds. As it is explained before in scenario 1, another vehicle is next to it, and it does not let the ego to reach its target position laterally.

47
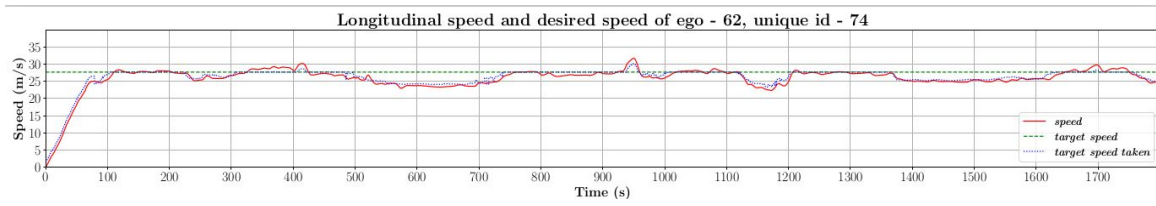
Figure 5.19: Longitudinal speeds representation for a density of 130 with weight equal to 1
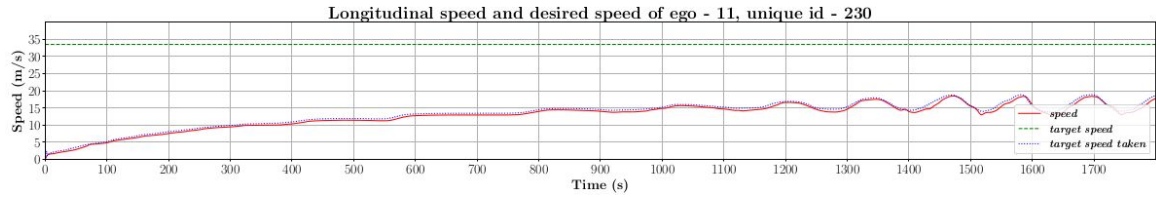

Figure 5.20: Longitudinal speeds representation for a density of 240 with weight equal to 1
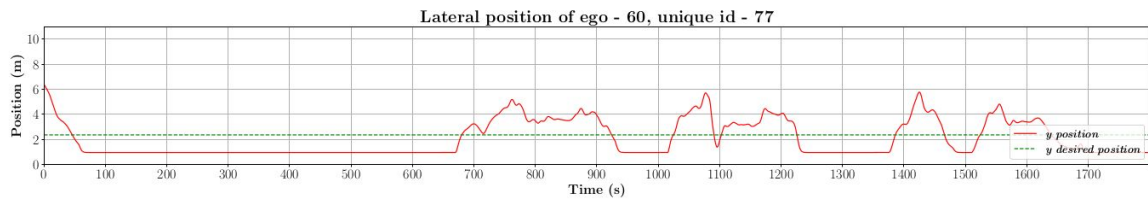
Figure 5.21: Lateral desired position behavior for a vehicle with weight equal to 1

From figure 5.21, it can be observed that between 50 s and 680 s, the vehicle stays on the right side of the desired lateral position, as a result of this, the desired lateral speed during the same period, is greater than the actual lateral speed. The vice-versa happens during the brief time where the vehicle goes left of the desired lateral position and can be easily seen from figure 5.22.
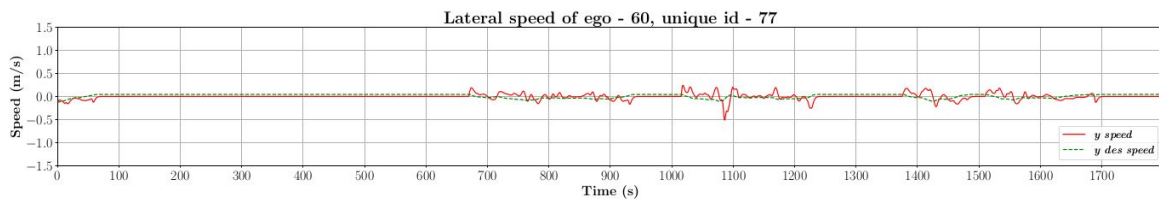
Figure 5.22: Lateral desired speed behavior for a vehicle with weight equal to 1

CHAPTER 6

CONCLUSION

The objective of this diploma thesis was the development of an LPS which is based on the premise "faster vehicles drive farther left". In the research done so far, the control strategy applied by [13] was setting the lateral desired speed equal to zero, to mitigate the unnecessary lateral movement. On the other hand, in this work, the LPS aims to distribute the vehicles in speed zones based on their longitudinal desired speed. First, the desired lateral position is defined linearly, based on the distribution of the longitudinal desired speeds. Afterwards, the desired lateral speed of each vehicle is calculated and applied in real-time, as it depends on its actual lateral position.

The main goal of this LPS is to improve the traffic flow for various traffic densities, while avoiding collisions. The proposed strategy was simulated for various densities and sufficient number of replications, in a lane-free environment using a custom-made extension, namely TrafficFluid-Sim, which is built for the Simulation of Urban MObility (SUMO) simulator, considering a 1 km ring-road.

For the investigation of the proposed strategy, two main scenarios were considered, one with only regular passenger vehicles, and one with both trucks and passenger vehicles. A base case set up in each scenario was considered for comparative analysis. In both scenarios a variety of densities have been tested, while different values of the weight for the lateral desired speed have been used. Moreover, several quantities, like the average traffic flow and statistical measures of the error in the lateral direction, are calculated for the evaluation of this method.

The results for the first scenario have shown, that the proposed LPS improves the traffic flow, mainly at densities around the critical density (200 veh/km), with the improvement at critical value reaching 7.47%. In low densities the vehicles have anyhow the essential space to move and to reach the longitudinal desired speeds, while for densities over the critical the traffic flow improvement is getting smaller, due to unavailability of enough space for maneuvers.

The results from the second scenario show, that the proposed LPS improves traffic flow in every density, with the best result of 15% achieved at the density of 240 veh/km. The improvement is attributed to the fact that the slow moving trucks are confined to the right-most part of the road, allowing the passenger cars to move with improved average speeds compared to base case. Whereas, in the base case, the trucks try more frequenty to overtake other slow moving trucks, and ultimately slow down the upstream passenger vehicles.

For both scenarios a variety of results in the form of tables and figures are presented for better illustration. Of course, in both cases, as the weight is increased, the vehicles are getting closer to their desired lateral position, something that is confirmed also by the statistical tools.

BIBLIOGRAPHY

[1] A. Ferrara, S. Sacone, and S. Siri, *Freeway traffic modelling and control.* Springer, 2018.

[2] R. I. Meneguette, R. De Grande, and A. Loureiro, "Intelligent transport system in smart cities," *Cham: Springer International Publishing*, 2018.

[3] M. Papageorgiou, K.-S. Mountakis, I. Karafyllis, I. Papamichail, and Y. Wang, "Lane-free artificial-fluid concept for vehicular traffic," *Proceedings of the IEEE*, vol. 109, no. 2, pp. 114–121, 2021.

[4] M. Schwenzer, M. Ay, T. Bergs, and D. Abel, "Review on model predictive control: an engineering perspective," *The International Journal of Advanced Manufacturing Technology*, vol. 117, no. 5, pp. 1327–1349, 2021.

[5] M. Rahman, M. Chowdhury, Y. Xie, and Y. He, "Review of microscopic lane-changing models and future research opportunities," *IEEE transactions on intelligent transportation systems*, vol. 14, no. 4, pp. 1942–1956, 2013.

[6] E. Marti, M. A. De Miguel, F. Garcia, and J. Perez, "A review of sensor technologies for perception in automated driving," *IEEE Intelligent Transportation Systems Magazine*, vol. 11, no. 4, pp. 94–108, 2019.

[7] J. Van Brummelen, M. O'Brien, D. Gruyer, and H. Najjaran, "Autonomous vehicle perception: The technology of today and tomorrow," *Transportation research part C: emerging technologies*, vol. 89, pp. 384–406, 2018.

[8] U. Montanaro, S. Dixit, S. Fallah, M. Dianati, A. Stevens, D. Oxtoby, and A. Mouzakitis, "Towards connected autonomous driving: review of use-cases," *Vehicle system dynamics*, vol. 57, no. 6, pp. 779–814, 2019.

[9] P. Thomas, A. Morris, R. Talbot, and H. Fagerlind, "Identifying the causes of road crashes in europe," *Annals of advances in automotive medicine*, vol. 57, p. 13, 2013.

[10] K. Goniewicz, M. Goniewicz, W. Pawłowski, and P. Fiedor, "Road accident rates: strategies and programmes for improving road traffic safety," *European journal of trauma and emergency surgery*, vol. 42, no. 4, pp. 433–438, 2016.

[11] M. Malekzadeh, I. Papamichail, M. Papageorgiou, and K. Bogenberger, "Optimal internal boundary control of lane-free automated vehicle traffic," *Transportation Research Part C: Emerging Technologies*, vol. 126, p. 103060, 2021.

[12] M. Malekzadeh, I. Papamichail, and M. Papageorgiou, "Linear–quadratic regulators for internal boundary control of lane-free automated vehicle traffic," *Control Engineering Practice*, vol. 115, p. 104912, 2021.

[13] V. K. Yanumula, P. Typaldos, D. Troullinos, M. Malekzadeh, I. Papamichail, and M. Papageorgiou, "Optimal path planning for connected and automated vehicles in lane-free traffic," in *2021 IEEE International Intelligent Transportation Systems Conference (ITSC)*, pp. 3545–3552, IEEE, 2021.

[14] V. K. Yanumula, P. Typaldos, D. Troullinos, M. Malekzadeh, I. Papamichail, and M. Papageorgiou, "Optimal path planning for connected and automated vehicles in lane-free traffic with vehicle nudging," *https://arxiv.org/abs/2207.09670*, 2022.

[15] M. Papageorgiou, M. Leibold, and M. Buss, "Optimierung. statische, dynamische, stochastische verfahren für die anwendung," Springer Berlin Heidelberg, 2015.

[16] M. Papageorgiou, M. Marinaki, P. Typaldos, and K. Makantasis, "A feasible direction algorithm for the numerical solution of optimal control problems-extended version," in *Chania, Greece: Technical University of Crete, Dynamic Systems and Simulations Laboratory*, pp. 2016–26, 2016.

[17] D. Q. Mayne and H. Michalska, "Receding horizon control of nonlinear systems," in *Proceedings of the 27th IEEE Conference on Decision and Control*, pp. 464–465, IEEE, 1988.

[18] D. Q. Mayne, "Model predictive control: Recent developments and future promise," *Automatica*, vol. 50, no. 12, pp. 2967–2986, 2014.

[19] D. Troullinos, G. Chalkiadakis, D. Manolis, I. Papamichail, and M. Papageorgiou, "Lane-free microscopic simulation for connected and automated vehicles," in *2021 IEEE International Intelligent Transportation Systems Conference (ITSC)*, pp. 3292–3299, IEEE, 2021.

[20] P. A. Lopez, M. Behrisch, L. Bieker-Walz, J. Erdmann, Y.-P. Flötteröd, R. Hilbrich, L. Lücken, J. Rummel, P. Wagner, and E. Wießner, "Microscopic traffic simulation using sumo," in *2018 21st international conference on intelligent transportation systems (ITSC)*, pp. 2575–2582, IEEE, 2018.

[21] K. Sjoberg, P. Andres, T. Buburuzan, and A. Brakemeier, "Cooperative intelligent transport systems in europe: Current deployment status and outlook," *IEEE Vehicular Technology Magazine*, vol. 12, no. 2, pp. 89–97, 2017.

[22] C. Diakaki, M. Papageorgiou, I. Papamichail, and I. Nikolos, "Overview and analysis of vehicle automation and communication systems from a motorway traffic management perspective," *Transportation Research Part A: Policy and Practice*, vol. 75, pp. 147–165, 2015.

[23] M. Papageorgiou, C. Diakaki, V. Dinopoulou, A. Kotsialos, and Y. Wang, "Review of road traffic control strategies," *Proceedings of the IEEE*, vol. 91, no. 12, pp. 2043–2067, 2003.

[24] R. Ponnaluri and P. Alluri, *Connected and Automated Vehicles: Developing Policies, Designing Programs, and Deploying Projects: From Policy to Practice.* Elsevier Science, 2021.

[25] S. E. Shladover, "Connected and automated vehicle systems: Introduction and overview," *Journal of Intelligent Transportation Systems*, vol. 22, no. 3, pp. 190–200, 2018.

[26] V. Milanés, D. F. Llorca, J. Villagrá, J. Pérez, C. Fernández, I. Parra, C. González, and M. A. Sotelo, "Intelligent automatic overtaking system using vision for vehicle detection," *Expert Systems with Applications*, vol. 39, no. 3, pp. 3362–3373, 2012.

[27] B. Vanholme, D. Gruyer, B. Lusetti, S. Glaser, and S. Mammar, "Highly automated driving on highways based on legal safety," *IEEE Transactions on Intelligent Transportation Systems*, vol. 14, no. 1, pp. 333–347, 2012.

[28] D. González, J. Pérez, V. Milanés, and F. Nashashibi, "A review of motion planning techniques for automated vehicles," *IEEE Transactions on intelligent transportation systems*, vol. 17, no. 4, pp. 1135–1145, 2015.

[29] I. Karafyllis, D. Theodosis, and M. Papageorgiou, "Nonlinear adaptive cruise control of vehicular platoons," *International Journal of Control*, pp. 1–23, 2021.

[30] K. Muhammad, A. Ullah, J. Lloret, J. Del Ser, and V. H. C. de Albuquerque, "Deep learning for safe autonomous driving: Current challenges and future directions," *IEEE Transactions on Intelligent Transportation Systems*, vol. 22, no. 7, pp. 4316–4336, 2020.

[31] D. Troullinos, G. Chalkiadakis, I. Papamichail, and M. Papageorgiou, "Collaborative multiagent decision making for lane-free autonomous driving," in *Proceedings of the 20th International Conference on Autonomous Agents and MultiAgent Systems*, pp. 1335–1343, 2021.

[32] P. Typaldos, I. Papamichail, and M. Papageorgiou, "Minimization of fuel consumption for vehicle trajectories," *IEEE transactions on intelligent transportation systems*, vol. 21, no. 4, pp. 1716–1727, 2020.

[33]